AFRL-RX-TY-TR-2008-4618

ADVANCED CATALYSIS TECHNOLOGIES: LANTHANUM CERIUM MANGANESE HEXAALUMINATE COMBUSTION CATALYSTS AND FLAT PLATE REACTOR FOR COMPACT STEAM REFORMERS

Aly H. Shaaban
Applied Research Associates
P.O. Box 40128
Tyndall Air Force Base, FL 32403

DECEMBER 2008

Final Report for 1 October 2003 – 31 December 2008

AIRBASE TECHNOLOGIES DIVISION
MATERIALS AND MANUFACTURING DIRECTORATE
AIR FORCE RESEARCH LABORATORY
AIR FORCE MATERIEL COMMAND
139 BARNES DRIVE, SUITE 2
TYNDALL AIR FORCE BASE, FL 32403-5323

NOTICE AND SIGNATURE PAGE

Using Government drawings, specifications, or other data included in this document for any purpose other than Government procurement does not in any way obligate the U.S. Government. The fact that the Government formulated or supplied the drawings, specifications, or other data does not license the holder or any other person or corporation; or convey any rights or permission to manufacture, use, or sell any patented invention that may relate to them.

This report was cleared for public release by the Air Force Research Laboratory, Materials and Manufacturing Directorate, Airbase Technologies Division, Public Affairs and is available to the general public, including foreign nationals. Copies may be obtained from the Defense Technical Information Center (DTIC) (http://www.dtic.mil).

REPORT NUMBER AFRL-RX-TY-TR-2008-4618 HAS BEEN REVIEWED AND IS APPROVED FOR PUBLICATION IN ACCORDANCE WITH ASSIGNED DISTRIBUTION STATEMENT.

//signature//
REZA SALAVANI; DR-III
Work Unit Manager

//signature//
SANDRA R. MEEKER; DR-IV
Chief, Deployed Base Systems Branch

//signature//
ALBERT N. RHODES, PhD.; DR-IV
Acting Chief, Airbase Technologies Division

This report is published in the interest of scientific and technical information exchange, and its publication does not constitute the Government's approval or disapproval of its ideas or findings.

REPORT DOCUMENTATION PAGE

Form Approved
OMB No. 0704-0188

PLEASE DO NOT RETURN YOUR FORM TO THE ABOVE ADDRESS.

1. REPORT DATE *(DD-MM-YYYY)*	2. REPORT TYPE	3. DATES COVERED *(From - To)*
31-DEC-2008	Final Technical Report	01-OCT-2003 -- 31-DEC-2008

4. TITLE AND SUBTITLE

Advanced Catalysis Technologies: Lanthanum Cerium Manganese Hexaaluminate Combustion Catalysts for Flat Plate Reactor for Compact Steam Reformers

5a. CONTRACT NUMBER

FA4819-07-D-0001

5b. GRANT NUMBER

5c. PROGRAM ELEMENT NUMBER

62102F

6. AUTHOR(S)

Shaaban, Aly H.

5d. PROJECT NUMBER

4915

5e. TASK NUMBER

D1

5f. WORK UNIT NUMBER

4915D14A

7. PERFORMING ORGANIZATION NAME(S) AND ADDRESS(ES)

Applied Research Associates, Inc.
P.O. Box 40128
Tyndall AFB, FL 32403

8. PERFORMING ORGANIZATION REPORT NUMBER

9. SPONSORING/MONITORING AGENCY NAME(S) AND ADDRESS(ES)

Air Force Research Laboratory
Materials and Manufacturing Directorate
139 Barnes Drive, Suite 2
Tyndall AFB, FL 32403-5323

10. SPONSOR/MONITOR'S ACRONYM(S)

RXQD

11. SPONSOR/MONITOR'S REPORT NUMBER(S)

AFRL-RX-TY-TR-2008-4618

12. DISTRIBUTION/AVAILABILITY STATEMENT

Distribution Statement A. Approved for Public release; distribution unlimited.

13. SUPPLEMENTARY NOTES

Ref AFRL/RXQ Public Affairs Case #09-018. Document contains color images.

14. ABSTRACT

This effort investigated the impact of thin film coated catalyst on fuel reforming, developed a substituted hexaaluminate combustion catalyst, and investigated its application in a compact steam reformer. Thin film coated catalyst impact on fuel reforming was investigated using catalytic cracking process. Two cracking catalysts and three reactor configurations were used to investigate both packed-bed and thin film catalyst coated reactors. For the combustion catalyst development, several substituted hexaaluminates were synthesized via a surfactant-mediated process and tested for their catalytic propane combustion activity. After calcination, catalyst surface areas were as high as $78 m^2/g$. The best catalysts contained lanthanum, cerium, and manganese, with $La_{0.6}Ce_{0.4}MnAl_{11}O_{19}$ representing optimum performance. A parallel plate catalytic combustion reactor was tested using the hexaaluminate catalyst in pellets and supported on FeCrAlloy metal foam. Both tests burned propane and JP-8 jet fuel with low pressure drop.

15. SUBJECT TERMS

Hexaaluminate, manganese, lanthanum, cerium, catalytic combustion, propane, JP-8, surfactant, Fecralloy, foam

16. SECURITY CLASSIFICATION OF:			17. LIMITATION OF ABSTRACT	18. NUMBER OF PAGES	19a. NAME OF RESPONSIBLE PERSON
a. REPORT	b. ABSTRACT	c. THIS PAGE			Reza Salavani
U	U	U	UU	40	19b. TELEPHONE NUMBER *(Include area code)*

Reset

Standard Form 298 (Rev. 8/98)
Prescribed by ANSI Std. Z39.18

TABLE OF CONTENTS

LIST OF FIGURES

LIST OF TABLES

ACKNOWLEDGEMENT

THE AUTHOR ACKNOWLEDGES AND THANKS MR. TIMOTHY J. CAMPBELL AND DR. FRED S. THOMAS FOR THEIR DEDICATED EFFORTS IN THE DEVELOPMENT OF THIN FILM CATALYSIS AND THE COMBUSTION CATALYST

Summary

The steam reforming reaction is fast and endothermic; therefore, the rate of hydrogen production in the steam reforming reactor is generally limited by the rate of heat transfer from the heat source. In the conventional packed-bed steam reformer reactor using an open-flame or radiant burner as the heat source, the rate of heat transfer is limited by wall film and bed resistances. Heat transfer can be effectively improved by replacing the burner/packed-bed system with parallel channels containing metal foam inserts alternately coated with combustion or reforming catalyst. In this approach heat is transferred by conduction directly from the source to the sink, allowing for faster hydrogen production in a more compact reactor design. This approach, however, requires the development of active, stable combustion catalysts that can be coated directly onto metal supports. Also, the combustion reactor must be able to develop a relatively flat temperature profile along the flow axis, to allow for adequate residence time of reactants in the heated section of the adjacent steam reforming channel.

Metal-substituted hexaaluminates research is currently active to develop several classes of catalysts from combustion catalysts for high temperature lean natural gas turbines in order to reduce NO_x emissions to reforming catalyst to convert diesel and kerosene to hydrogen rich gases. Unlike standard γ-alumina catalyst supports, hexaaluminates maintain substantial surface areas at temperatures exceeding 1000 °C and thus are well-suited for high temperature catalytic combustion. They have the general formula $AM_xAl_{12-x}O_{19,}$ where A is a large cation from the alkaline earth metals or the lanthanides, and M is a transition metal cation close in size to the Al^{3+} cation. The A cation creates a layered structure which inhibits sintering while the M cation catalyzes combustion.

This effort investigated the impact of thin film coated catalyst on fuel reforming, developed a substituted hexaaluminate combustion catalyst, and investigated its application in a compact steam reformer. Thin film coated catalyst impact on fuel reforming was investigated using catalytic cracking process. Two cracking catalysts and three reactor configurations were used to investigate both packed-bed and thin film catalyst coated reactors. For the combustion catalyst development, several substituted hexaaluminates were synthesized via a surfactant-mediated process and tested for their catalytic propane combustion activity. After calcination, catalyst surface areas were as high as $78m^2/g$. The best catalysts contained lanthanum, cerium, and manganese, with $La_{0.6}Ce_{0.4}MnAl_{11}O_{19}$ representing optimum performance. A parallel plate catalytic combustion reactor was tested using the hexaaluminate catalyst in pellets and supported on FeCrAlloy metal foam. Both tests burned propane and JP-8 jet fuel with low pressure drop.

1. INTRODUCTION

Mobile Electric Power (MEP) is one of five essential infrastructure elements in Tri-service deployments. The Army Force Providers and the Air Force Bare Bases are examples of Tri-service extensive use of MEP generators. Fuel cell electric power generators promise to provide significant advantages over conventional diesel generator sets for mobile electric power applications. They can provide power with higher fuel efficiency and higher reliability; they are quieter; and with the development of a compact fuel processor, they can have smaller footprint. The fuel processor, using steam reforming, converts hydrocarbon fuels to a suitable fuel for the fuel cell stack.

The steam reforming reaction is fast and endothermic; therefore, the rate of hydrogen production in the steam reforming reactor is generally limited by the rate of heat transfer from the heat source. In the conventional packed-bed steam reformer reactor, using an open-flame or radiant burner as the heat source, the rate of heat transfer is limited by wall film and packed-bed thermal resistances. The necessity to attain high performance with high degree of compactness together in one unit has led to the development of technologies to minimize thermal resistance. In pursuit of these technologies, thin film catalysis in flat parallel plate configured reactors has the potential to achieve these goals. The flat plate reactor is a stack of alternating catalyst coated combustion-reforming channels where heat is transferred by conduction directly from the source to the sink, allowing for faster hydrogen production in a more compact reactor design [1]. This approach, however, requires the development of active, stable combustion catalysts that can be coated directly onto metal supports. Also, the combustion channels must be able to develop a relatively uniform temperature profile along the flow axis, to allow for adequate residence time of reactants in the heated section of the adjacent steam reforming channel.

Metal-substituted hexaaluminates research is active in developing several classes of catalysts from combustion catalysts for high temperature lean natural gas turbines, in order to reduce NO_x emissions, to reforming catalyst to convert distillate fuels, such as diesel and kerosene, to hydrogen rich gases [2–22]. The growing importance of hexaaluminates is due to its refractory properties which give them high thermal stability. Unlike standard γ-alumina catalyst supports, they maintain substantial surface areas at temperatures exceeding 1000 °C and thus are well-suited for high temperature catalytic combustion. In this effort, catalytically active elements are doped directly into the hexaaluminate lattice, resulting in active sites that are both isolated and well-dispersed. They have the general formula $AM_xAl_{12-x}O_{19,}$ where A is a large cation from the alkaline earth metals or the lanthanides, and M is a transition metal cation close in size to the Al^{3+} cation. The A cation creates a layered structure which inhibits sintering while the M cation catalyzes combustion.

This effort investigated the impact of thin film coated catalyst on the performance of fuel reforming processes, developed a substituted hexaaluminate combustion catalyst, and investigated its application in a compact steam reformer. Thin film coated catalyst impact on the performance of fuel reforming was investigated using catalytic cracking process. The cracking process was proposed as a pre-reforming step to remove sulfur content of the fuel. Two cracking catalysts and three reactor configurations were used to investigate both packed-bed and thin film catalyst coated reactors and facilitate comparison.

In the development of combustion catalyst, several substituted hexaaluminates were synthesized via a surfactant-mediated process and tested for their catalytic propane combustion activity. After calcination, catalyst surface areas were as high as $78 m^2/g$. Test results showed that the best catalysts contained lanthanum, cerium, and manganese, while the catalyst with the formula $La_{0.6}Ce_{0.4}MnAl_{11}O_{19}$ gave optimum performance.

The combustion catalyst was tested in a parallel plate catalytic combustion reactor using the hexaaluminate catalyst both in pellet form and supported on metal foam. Both tests burned propane and JP-8. Low pressure drop, a sufficiently-uniform temperature profile, and stable self-sustained operation have been achieved. Suitable metal foam substrates are, in particular, those produced from alloys of iron, nickel and chromium, or those produced from alloys of iron, chromium, aluminum and cobalt, such as those marketed under the trademark of Kanthal, or those produced from alloys of iron, chromium, aluminum and yttrium, marketed under the trademark of FeCrAlloy, or those produced from alloys of iron, chromium, and aluminum under trademark of Recemat. Depending on temperature range, the metal may also be a simple carbon steel, or cast iron.

2. OBJECTIVES

The main goal was to develop flat plate technology for a compact fuel processor. In achieving this goal, three objectives have been accomplished. The first was the determination of the impact of catalyst coating on the performance of fuel processing, and the second was the development of a combustion catalyst that could withstand the intense heat generated during logistic fuel combustion while maintaining substantial surface area per unit volume; while the third was the achievement of high heat flux with uniform temperature profile along the flow axis, to allow for adequate residence time of reactants.

3. RESEARCH PROGRAM

3.1 Research Basis

Steam reforming is an endothermic process that efficiently reforms heavier hydrocarbons, such as military logistic fuels (JP4, JP5, JP8, and JP100), kerosene, diesel, synthetic fuels, and other hydrocarbon fuels into hydrogen rich gas for fuel cell use. Maximum reaction intensity is obtained when heat flux into reaction sites is maximized. Therefore, a compact steam reforming technology requires minimum thermal resistance to achieve high heat flux.

Packed-bed reactors have inherently severe heat transfer limitations. In the conventional packed-bed reactor and burner combination, thermal energy is mainly transferred from the burner to the outer surface of the packed-bed reactor by radiation then by conduction through reactor walls and catalyst bed, encountering severe thermal resistance in the catalyst bed. Heat transfer can be effectively improved by replacing the conventional burner/packed bed system with a flat plate reactor configuration, with parallel channels alternately coated with thin film combustion or reforming catalyst [1]. As shown in Figure 1, in flat plate configuration, heat is transferred by conduction directly from the heat source to the reaction sites, allowing for faster

hydrogen production in a more compact reactor design. In this approach the conventional packed-bed thermal resistance is eliminated allowing for maximum heat flux and a reactor design operating at its optimum operating temperatures. This approach, however, requires the development of active and stable combustion catalysts that can be coated directly onto metal supports. Furthermore, the combustion channel must be able to develop a relatively uniform temperature profile along the flow axis, to allow for adequate residence time of reactants in the heated section of the adjacent steam reforming channel.

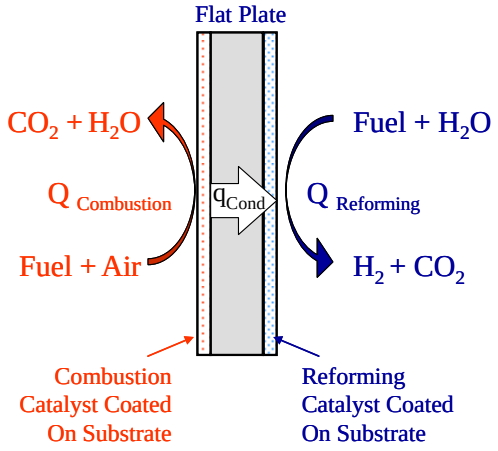

Figure 1: Flat Plate Reactor Concept

3.2 Thin Film Coated Catalyst Proof of Concept

In an effort to investigate the impact of thin film catalysis on the reaction intensity, the catalytic cracking process was chosen, since it was identified as a process step to remove fuels' sulfur content [23]. In the study, JP-8 catalytic cracking conversion was measured at atmospheric pressure and at temperatures and space velocities appropriate for use in compact fuel processor systems. To facilitate effective comparison, two different catalyst types were tested in two packed bed tubular reactors and two coated-wall tubular reactors.

3.2.1 Experimental Effort

3.2.1.1 Catalyst Preparation: The two cracking catalysts studied were acidic zeolite catalysts, which are often used in fluidized catalytic cracking (FCC) processes, and a Mn/alumina formulation that has been reported in the literature to give high light fractions yield with low selectivity to coke [24]. ZSM-5 type (MFI) zeolite (Zeolyst CBV5524G, SiO_2/Al_2O_3 ratio of 50, NH_4^+ cation, 0.05 wt.% Na_2O, 425 m^2/g surface area) and Beta type (BEA) zeolite (Zeolyst CP814E, SiO_2/Al_2O_3 ratio of 25, NH_4^+ cation, 0.05 wt.% Na_2O, 680 m^2/g surface area) were obtained from the vendor as extrudate pellets. The extrudate pellets were ground and dry-sieved to 12-16 mesh particles, then activated by calcining in air at 450°C for 4 hours. Mn/alumina catalyst was prepared by wet impregnation of 8-14 mesh γ-alumina particles with a solution of manganese electrolytic metal in nitric acid, followed by drying at 90°C for 30 minutes and calcining in air at 450°C for 4 hours. The final manganese metal loading was 11 wt%, and the as-prepared Mn/γ-alumina catalyst pellets had specific surface area of 151 m^2/g.

TABLE 1: Dimensions and Properties of Tubular Cracking Reactors

Reactor	Type	Catalyst	OD (cm)	ID (cm)	$V_{reactor}$ (cm^3)
MnAl-PB	Packed bed	Mn/γ-alumina	0.635	0.478	5.47
MFI/BEA-PB	Packed bed	Mixed zeolites, 1:1 MFI:BEA	0.635	0.478	5.47
BEA-CW1	Coated wall, 1 channel	BEA zeolite	0.318	0.160	0.61
BEA-CW2	Coated wall, 2 channels	BEA zeolite	0.318	2 x 0.102	0.50

In Table 1, the properties and dimensions of the four tubular reactors studied are listed: outer diameter (OD), inner diameter (ID) and reactor volume ($V_{reactor}$). All reactor tubes were 30.5 cm long and consisted of high-alumina ceramic tubes (McMaster-Carr Supply Co.). The densities of the packed beds were 0.98 and 0.58 g/cm^3 for the Mn/γ-alumina and mixed zeolites, respectively.

Coated wall reactors were prepared by pretreating the tube's inner surface with 10 wt.% nitric acid, then washcoating with a suspension containing 20 wt.% finely-ground BEA zeolite powder and 0.6 wt.% sodium silicate (Ludox AS-40, Aldrich). After washcoating, the tubes were dried at 200°C for 30 minutes, and then calcined in air 400°C for 16 hours. The coated catalyst layers were activated by exchanging with 1M NH_4NO_3 for 16 hours, then dried at 90°C for 30 minutes, followed by calcining in air at 450°C for 4 hours. The coating procedure used was adapted from a procedure reported previously for coating BEA zeolites on cordierite monoliths [25]. Figure 2 shows a cross-section of a packed-bed tube reactor and the cross-section of the 2-channel coated wall tube reactor.

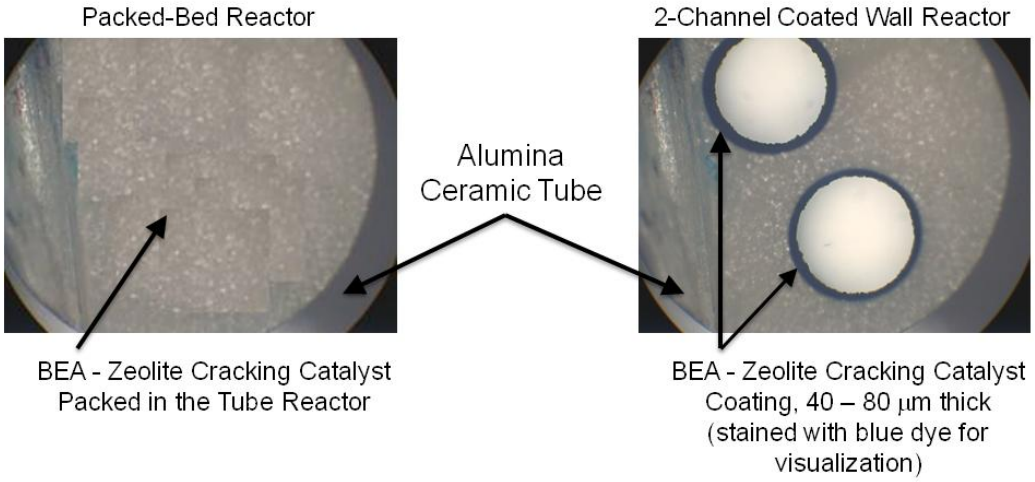

Figure 2: Alumina Ceramic Tube Packed-Bed and 2-Channel Coated Wall Reactors

3.2.1.2. Test Apparatus: Figure 3 is a diagram of the experimental apparatus used to test the performance of the tubular cracking reactors. JP-8 feed from a syringe

pump with ± 1% volumetric accuracy (Isco model LC-5000) was sent through a preheater that consisted of a 406 cm long, 0.318 cm OD, 0.216 cm ID section of silcosteel-treated stainless steel tubing (Restek Corp.), wound into a coil 3 cm in diameter, 28 cm long. This tube coil was clamped within a radiant tube heater, 5.1 cm ID, 735 watts maximum power (Omega). The exterior temperature of the preheater tube at the inlet end of the coil ($T_{coil,in}$) was monitored using a type-E thermocouple. Preheater power was controlled with a variable voltage power supply (Staco, 0-140V), and adjusted to maintain the tube exterior at the hot end of the coil ($T_{coil,ex}$) at 610 ± 5°C, which was monitored using a type-E thermocouple positioned near the tube. Preheated JP-8 flowed out of the tube coil, passed a type-E thermocouple, which measured the reactor feed temperature (T_{feed}), and into the reactor tube. The reactor tube was heated using an approximately 90 cm long piece of 28 AWG Ni/Cr heating wire wrapped tightly around the outside of the tube, with a sleeve of insulation covering over the tube and wire. Reactor heating power was controlled with a second variable voltage power supply. Flow exiting the reactor tube passed another type-E thermocouple which monitored the product stream temperature ($T_{product}$), then through an air-cooled coil of Silcosteel tubing, 0.318 cm OD, 0.216 cm ID, 80 cm L, where any condensable products were condensed to liquid. Liquid residue was separated using a gas/liquid separator with < 1 cm^3 hold-up volume, and collected in a removable glass screw-top vial connected to the bottom of the separator. Light gas product exited the top of the separator and passed a septum fitting sample port before being vented to a fume hood. Overall system pressure was monitored using a pressure transducer in the syringe pump, and was < 10 psig (panels per square inch) throughout all experiments.

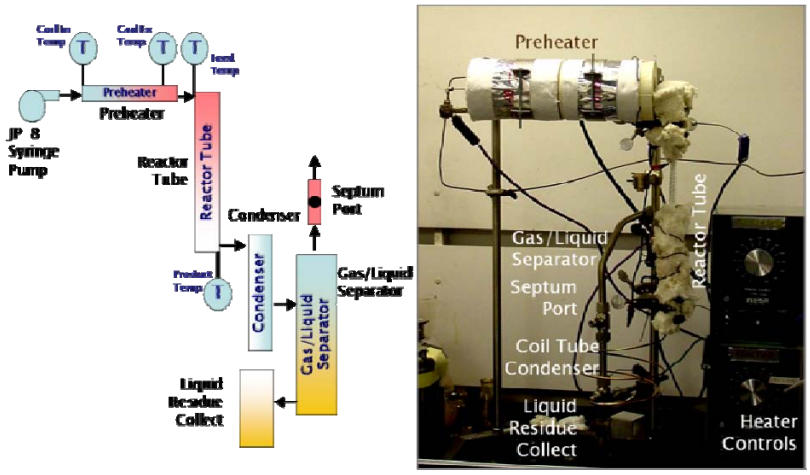

Figure 3: JP-8 Catalytic Cracking Experimental Setup

Steady-state cracking conversion was determined by first establishing a specified JP-8 feed rate (Q_{Feed}, cm^3/min) with the syringe pump, then bringing the preheater up to operating temperature, then heating the reactor tube to achieve a steady $T_{Product}$ temperature. After allowing about 10 minutes for the system to stabilize, a weighted collection vial was connected to the gas/liquid separator, and liquid residue was collected for a measured collection time (Δt, minutes). The vial was then removed and reweighed to determine the mass of liquid residue (m_{Liquid}) collected. The cracking conversion was then calculated as:

$$Conversion\ \ (wt.\%) = 100\left(1 - \frac{m_{Liquid}}{Q_{Feed}\,\Delta t\ \ \rho^{JP-8}}\right) \qquad (1)$$

Where ρ^{JP-8} is the density of the JP-8 feed, which was measured to be 0.792 ± 0.002 g/cm^3. During the run, two samples of the cracked gas were drawn through the septum port using a gas-tight syringe and analyzed using the gas chromatographic methods described below. The liquid residue sample was also analyzed by gas chromatography as described below.

3.2.2 Results and Discussion

3.2.2.1 Preheater Performance: Heat transfer in the preheater coil increased with increasing JP-8 flow rate as shown in Figure 4. The temperature of the JP-8 entering the preheater coil from the syringe pump was 24 ± 2°C. At Q_{Feed} = 0.5 mL/min, T_{Feed} remained below 200°C, which means that the fuel was only partly vaporized at this feed rate, given that the typical boiling range of JP-8 is from about 180 to 270°C [26]. Increasing $T_{Coil,Ex}$ to greater than 620°C caused pyrolytic cracking and coking to occur in the preheater tube coil, which would have confounded the experimental results. When $T_{Coil,Ex}$ was maintained at less than 620°C, cracking conversion in the preheater was less than 5 wt.%. Using reported properties of JP-8 [26] and the data in Figure 4, the average inner heat transfer coefficient for the preheater tube coil was estimated to be 0.2, 1.5, 5.6, and 15 W/m^2°C at Q_{Feed} of 0.5, 1.0, 2.0, and 4.0cm^3/min, respectively. Better heat transfer in the preheater could have been achieved over the same range of flow rates by using smaller ID tubing; however, tests with JP-8 vaporization in tubes smaller than 0.2 cm ID showed that they are prone to plugging during minor system upsets such as flow rate changes. The 0.216-cm ID preheater tube coil was operated with $T_{Coil,Ex}$ = 610°C for more than 40 hours without any measurable increase in back pressure. Heat transfer in the coil was observed to increase slightly during testing, so that at Q_{Feed} of 1.0 cm^3/min T_{Feed} was initially < 260°C, but after 30 hours of use T_{Feed} had increased to > 290°C at the same flow rate.

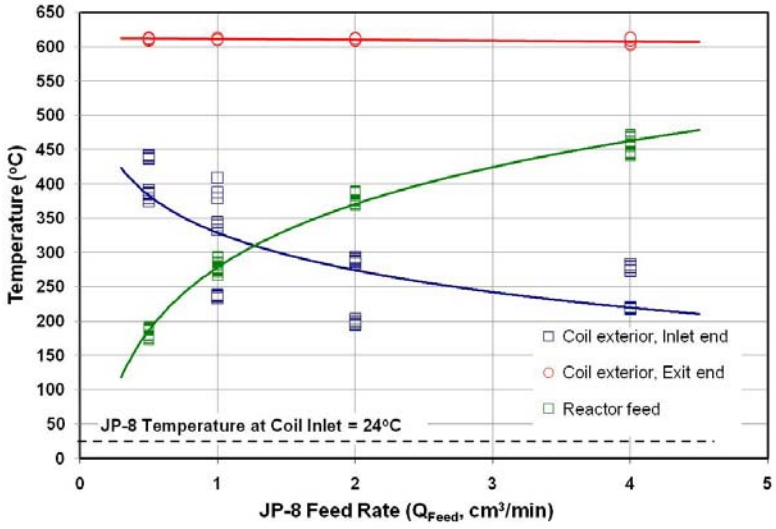

Figure 4: JP-8 heating in the 406-cm L x 0.216-cm ID preheater tube coil.

3.2.2.2. Reactor Performance: For practical application in compact fuel processor systems, catalytic cracking reactors must be small in size and thermally efficient. Small cracking reactor size can be achieved if high fuel cracking conversion rate can be obtained while operating the reactor at high space velocities, while thermal efficiency requires that the reactor operates at as low a temperature as possible. JP-8 cracking conversion in the packed bed catalytic reactors MNAL-PB and MFI/BEA-PB is shown in Figure 5. Conversion is plotted against mean reactor temperature to compensate for small increases in T_{Feed} during testing. The JP-8 feed rate is expressed as liquid hourly space velocity (LHSV), which is calculated as:

$$LHSV\ \left(h^{-1}\right) = \frac{60\,Q_{Feed}}{V_{\text{Reactor}}} \qquad (2)$$

where $V_{Reactor}$ is the reactor tube internal volume (see Table 1). For both packed-bed reactors, isothermal operation (i.e., $T_{Product} \approx T_{Feed}$) at any space velocity yielded < 10 wt% conversion. As heating power to the reactor was increased, conversion increased sharply with increasing $T_{Product}$. At each space velocity and temperature, the MFI/BEA-PB reactor produced slightly greater conversion than the MnAl-PB reactor. The greater performance of the MFI//BEA-PB reactor could be due to greater activity of the mixed zeolites catalyst compared to the Mn/γ-alumina, or could be due to better heat transfer due to the slightly smaller particle size and more irregular particle shape of the zeolites.

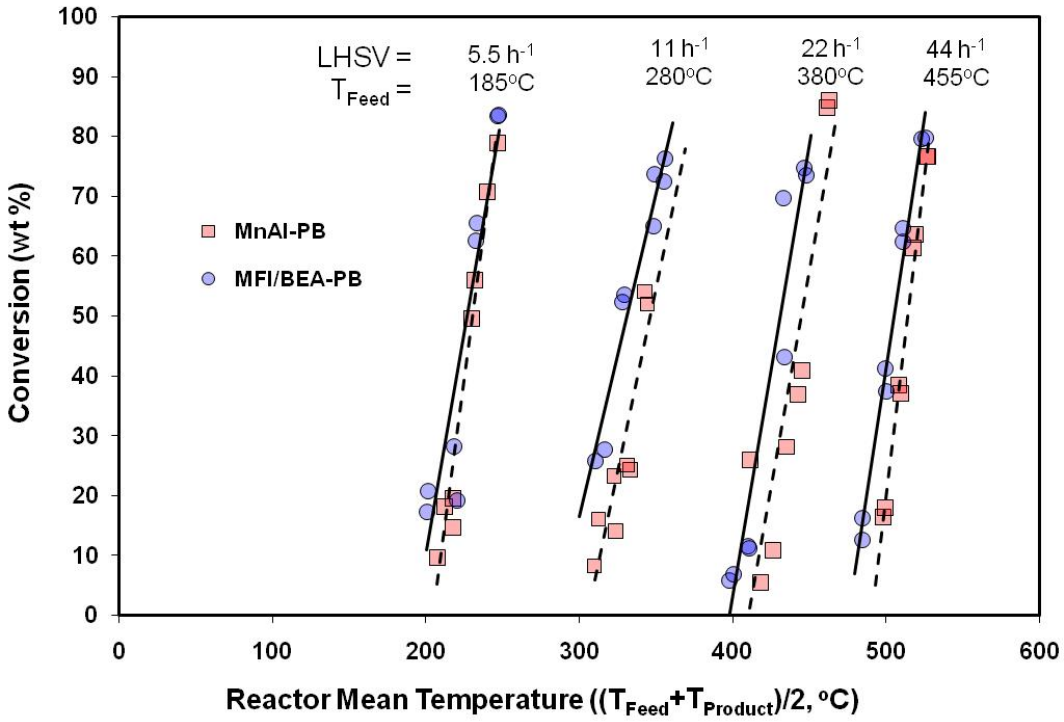

Figure 5: Effects Of Reactor Temperature and Space Velocity On Cracking Conversion In Packed-bed Reactors.

Catalytic cracking of hydrocarbons is an endothermic process, and the endotherm of JP-8 catalytic cracking has been measured to be approximately 930 J/g at 80 vol% conversion [27]. The performance of a catalytic cracking reactor can be limited by the catalyst activity, by the rate of heat transfer to the catalyst surface, or by the rate of mass transfer of reactants and products to and from the catalyst surface. Flow conditions in these experiments were chosen to provide low pressures to simulate conditions using the small, lightweight fuel pumps required in compact fuel processors. These flow conditions, however, also yield low Reynolds numbers, and limited heat and mass transfer rates. Heat transfer to the catalyst surface could be improved by coating the catalyst material directly on the inner wall of the heated tube, rather than using a packed-bed of catalyst particles.

Improved heat transfer using thin layers of catalysts coated on reactor walls has been reported for endothermic processes such as methane steam reforming [1] and ethane dehydrogenation [28]. Figure 6 shows the results obtained using reactors BEA-CW1 and BEA-CW2 at LHSV = 100 h^{-1}. Both coated tubes had outer diameters of 0.318 cm, but BEA-CW1 had a single inner channel 0.160 cm in diameter, while BEA-CW2 had two parallel inner channels each 0.102 cm in diameter. Comparison of Figures 5 and 6 shows that BEA-CW1 produced 80 wt% conversion at < 500^{o}C mean temperature, while both packed-bed reactors required a mean temperature of > 520^{o}C to give the same conversion at less than half the space velocity. BEA-CW2 produced 80 wt% conversion at < 380^{o}C mean reactor temperature (T_{Feed} = 253^{o}C, $T_{Product}$ = 500^{o}C) and 100 h^{-1} LHSV. These results demonstrate that high JP-8 cracking conversion at high space velocity can be achieved at low pressures and moderate reactor temperatures using coated wall catalytic reactors.

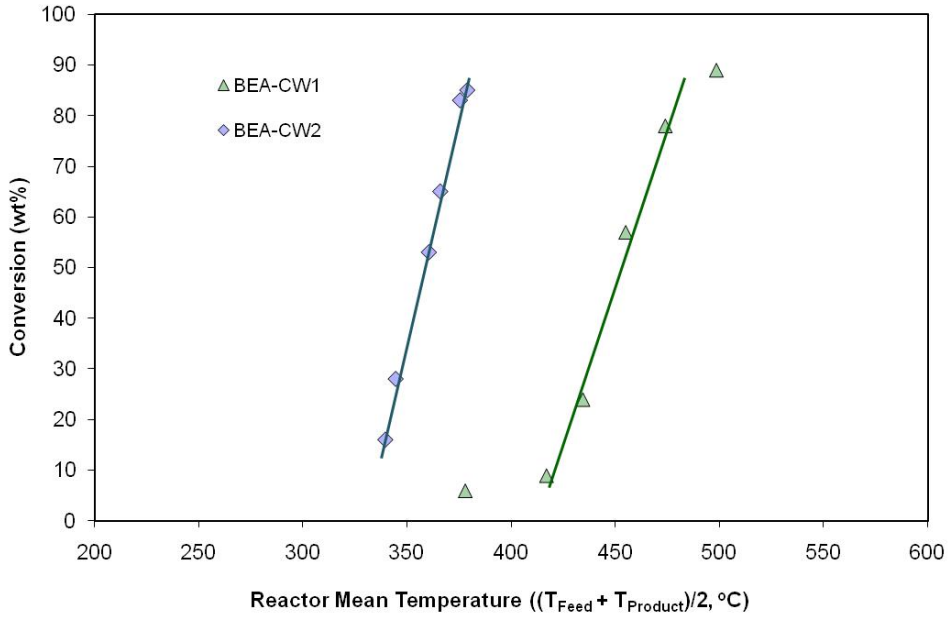

Figure 6: Effect Of Reactor Temperature On Cracking Conversion In Coated Wall Reactors At LHSV = 100 h^{-1}

Figure 7 shows a comparison between packed-bed and catalyst coated reactors' data. The thin film coated two channel reactor data at $100h^{-1}$ are shown along with three packed-bed MFI/BEA-PB data sets, for 11, 22, and $44h^{-1}$. The catalyst coated reactor performed superior to the packed-bed, requiring lower operating temperatures and higher space velocity to achieve the same conversion efficiencies. The thin film coated reactor performance at $100h^{-1}$ lay between the packed-bed performance at 11 h^{-1} and 22 h^{-1}. To facilitate a closer comparison, the packed-bed and thin film reactors' data sets were interpolated using *Multi–Polynomial Regression* technique to calculate a LHSV for the packed-bed reactor that matches the operating mean temperatures and cracking conversion efficiency of the thin film catalyst coated reactor (Appendix A). A polynomial of a fifth degree was selected and a LHSV of $14.86h^{-1}$ was calculated, raising the potential for coated catalyst reactors to process more than six times the amount of fuel in a similar volume, for the same conversion efficiencies, and at similar temperature range as a packed-bed reactor.

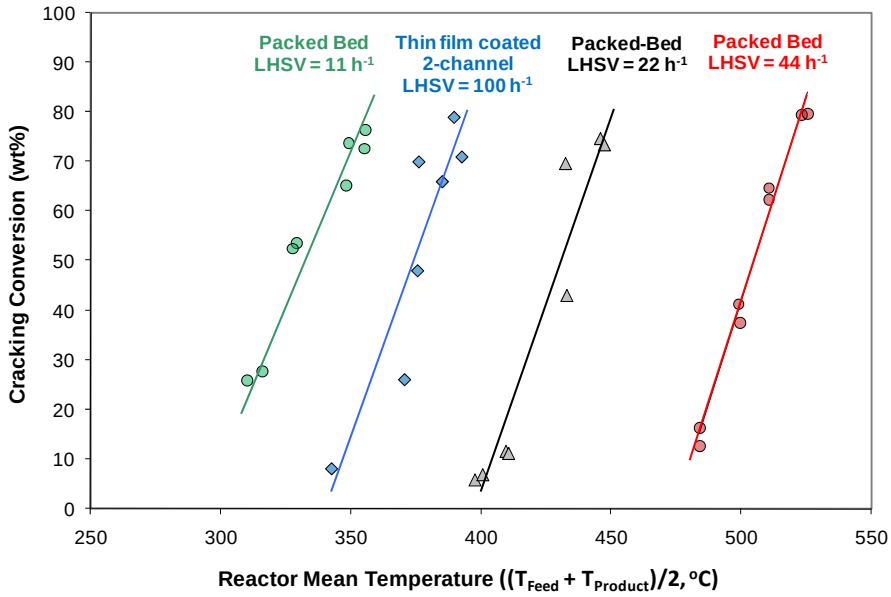

Figure 7: Comparison between Packed-Bed MFI/BEA-PB and Catalyst Coated Reactors

3.3 Combustion Catalyst Development

In this effort the combustion catalyst was developed and initially tested in a packed-bed reactor to evaluate its performance.

3.3.1 Experimental Procedure and Development Effort

3.3.1.1. Catalyst Preparation: Catalysts were synthesized using a modified surfactant-mediated procedure devised by Cho *et al.* [16]. Stoichiometric quantities of acetates of the A and M ions (Aldrich) and 10 grams cetyltrimethylammonium chloride (25wt. % in water, Aldrich) were mixed together. 25 grams of alumina sol (10 % Al_2O_3, 10-100 nm, Nissan, colloidal aqueous alumina) gradually stirred in at a rate of 2.5 grams every 2 minutes. 15

grams urea (Fisher) was added, followed by stirring for 15 minutes and ultrasonic agitation for one hour. The mixture was heated at 100°C for 24 hours to decompose the urea into carbon dioxide and ammonia. This increased the pH and caused sol condensation. The mixture was calcined in air at 550°C overnight and at 1100 °C for 6 hours to form the hexaaluminate, drive off the ammonia, and burn off the surfactant and acetate. The specific surface area of this catalyst when first prepared was 78 m^2/g; as measured by N_2-BET on a Micromeritics Flowsorb 2300.

3.3.1.2. Test Apparatus: The catalysts were evaluated in a packed-bed reactor made of a 30.5 cm long, 0.64 cm OD, and 0.48 cm ID alumina tube heated by a tube furnace. To measure the light-off curves, the reactor was fed 94sccm air, 3sccm propane, and 3sccm neon. Combustion gas samples were taken through a septum downstream of the furnace and analyzed by gas chromatography using a 30 meter Carboxen 1010 PLOT column (Supelco), argon carrier gas, and a thermal conductivity detector. The neon in the gas mixture provided an internal standard to correct for detector drift and variation in injection volume. One catalyst formulation ($LaMnAl_{11}O_{19}$) was tested for stability by increasing the packed-bed gas flows to 238sccm air and 10sccm propane. A Kanthal heating wire wrapped around the reactor initiated self-sustained catalytic combustion. Light-off curves with a feed of 94sccm air, 3sccm propane, and 3sccm neon were acquired both before and after the test to detect catalyst deactivation.

3.3.2 Results and Discussion

Substituted hexaaluminate catalysts and their surface area measurements are listed in Table 2. As transition metal substitution increases, surface area tends to decrease. For x = 0.5 transition metal cations per hexaaluminate unit, surface area ranges from 65 to 78 m^2/g; for x = 1 surface area ranges from 46 to 70 m^2/g; for x =2 surface area ranges from 27 to 62 m^2/g; and the catalyst with x = 3 has a surface area of 12 m^2/g. This is consistent with other results in the literature. Artizzu-Duart *et al*. [7] found that surface area declined from 14–20 m^2/g for x = 1 to 6–10 m^2/g for x = 4. Likewise, Wang *et al*. [17] reported that surface area declined from 49 m^2/g for x = 0 to 7 m^2/g for x = 6. Transition metal-catalyzed sintering has been proposed as the cause of this phenomenon [16, 17].

Table 2 also lists temperatures for 50% and 100% conversion, donated by T_{50} and T_{100}, and partial oxidation products for the light-off curves depicted in Figures 8–11. Figure 8 compares the performance of substituted hexaaluminate catalysts that have previously been reported in the literature. Figure 9 shows the effect of substituting cerium for manganese in $LaMnAl_{11}O_{19}$. Figure 10 shows the effect of substituting cerium for lanthanum in $LaMnAl_{11}O_{19}$. Figure 11 shows light-off curves for $LaMnAl_{11}O_{19}$ used in high-temperature stability test.

In general, catalysts with 1–3 manganese cations per hexaaluminate unit are most active. They have the lowest light-off temperatures and completely oxidize propane to carbon dioxide and water. Its high manganese content provides a higher intrinsic activity than the other catalysts and thus the lowest T_{50}. Specific surface area plays a major role in catalyst performance. Near full conversion, mass transfer limitations between the gas bulk and the catalyst surface impact conversion process, catalysts with low specific surface areas will have their light-off curves lagging behind those with high specific surface areas.

Catalysts with 0.5 manganese cations per hexaaluminate unit are less active. $LaCo_{0.5}Mn_{0.5}Al_{11}O_{19}$ and $LaMg_{0.5}Mn_{0.5}Al_{11}O_{19}$ reach full conversion at temperatures about 80°C higher than the best catalysts. $La_{0.5}Mn_{0.5}Al_{11}O_{19}$ is competitive with catalysts with twice its manganese content because of its exceptionally high surface area. For all three catalysts, combustion is incomplete. Even when propane is completely consumed, hydrogen is present in the exhaust. The catalysts without manganese are poor. They have high light-off temperatures and produce substantial amounts of hydrogen, carbon monoxide, and ethylene as partial oxidation products. Of the metals tested, iron is best, followed by cobalt and cerium.

Our results concur with Wang *et al.* [17] and Jang *et al*. [4], who also found that $LaMnAl_{11}O_{19}$ was the best hexaaluminate combustion catalyst, neglecting for the moment, catalysts with cerium substitution for lanthanum, which have not yet been reported in the literature. Our $LaMg_{0.5}Mn_{0.5}Al_{11}O_{19}$ did not perform nearly as well as that of Groppi *et al*., which marginally outperformed $LaMnAl_{11}O_{19}$ [18]. Our bimetallic manganese-cobalt catalyst was similarly lacking and did not exhibit the synergy reported by Yan and Thompson [3].

TABLE 2: Catalyst Surface Area and Propane Light-Off Performance

Catalyst	**Specific Surface Area (m^2/g)**	**T_{50} (°C)**	**T_{100} (°C)**	**Partial Oxidation Products**
$La_{0.6}Ce_{0.4}MnAl_{11}O_{19}$	64	320	370	-
$La_{0.5}Ce_{0.5}MnAl_{11}O_{19}$	67	330	380	-
$La_{0.8}Ce_{0.2}MnAl_{11}O_{19}$	62	340	390	-
$La_{0.7}Ce_{0.3}MnAl_{11}O_{19}$	57	340	390	-
$BaMn_3Al_9O_{19}$	12	345	420	-
$LaMnAl_{11}O_{19}$	53	350	400	-
$BaMnAl_{11}O_{19}$	62	355	410	-
$La_{0.9}Ce_{0.1}MnAl_{11}O_{19}$	61	355	410	-
$LaMn_{0.95}Ce_{0.05}Al_{11}O_{19}$	57	365	410	-
$Sr_{0.8}La_{0.2}MnAl_{11}O_{19}$	70	375	410	-
$BaFeMnAl_{10}O_{19}$	27	375	410	-
$La_{0.5}Mn_{0.5}Al_{11}O_{19}$	78	365	410	H_2
$LaMn_{0.7}Ce_{0.3}Al_{11}O_{19}$	63	365	430	H_2
$LaMn_{0.5}Ce_{0.5}Al_{11}O_{19}$	59	385	450	H_2
$LaCo_{0.5}Mn_{0.5}Al_{11}O_{19}$	67	390	450	H_2
$LaMg_{0.5}Mn_{0.5}Al_{11}O_{19}$	65	400	460	H_2
$BaFe_2Al_{10}O_{19}$	62	435	480	H_2, CO, C_2H_4
$LaMn_{0.05}Ce_{0.95}Al_{11}O_{19}$	59	470	520	H_2, CO, C_2H_4
$LaCoAl_{11}O_{19}$	46	480	530	H_2, CO, C_2H_4
$BaCe_3Al_9O_{19}$	44	480	530	H_2, CO, C_2H_4

To improve upon $LaMnAl_{11}O_{19}$, we experimented with cerium substitution. Cerium substitution for manganese has been shown to augment manganese oxide catalysts. For the wet oxidation of ammonia, a manganese/cerium ratio of 7:3 was optimal [19]. For the wet oxidation of ethylene glycol, a manganese/cerium ratio of 1:1 was optimal [20, 21]. A manganese/cerium ratio of 6:4 was best for the wet oxidation of phenol [22]. However, our results show that partially replacing manganese with cerium in $LaMn_{1-x}Ce_xAl_{11}O_{19}$ actually reduces catalytic activity, Figure 8. It is interesting to note that the light-off curves for $LaMn_{0.5}Ce_{0.5}Al_{11}O_{19}$ and $LaCo_{0.5}Mn_{0.5}Al_{11}O_{19}$ are nearly identical and that in the absence of manganese, cobalt- and cerium-substituted hexaaluminates are equivalent catalysts. It thus appears that cerium and cobalt merely dilute manganese without providing any synergistic effects.

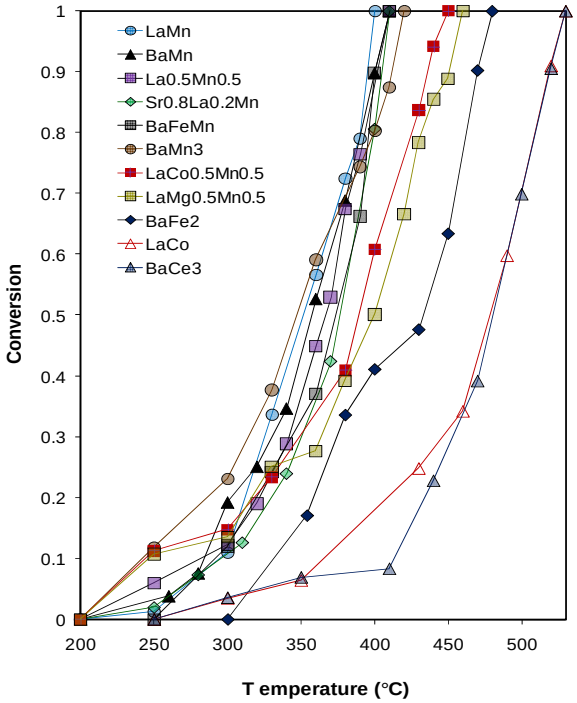

Figure 8: Light-off curves for propane combustion

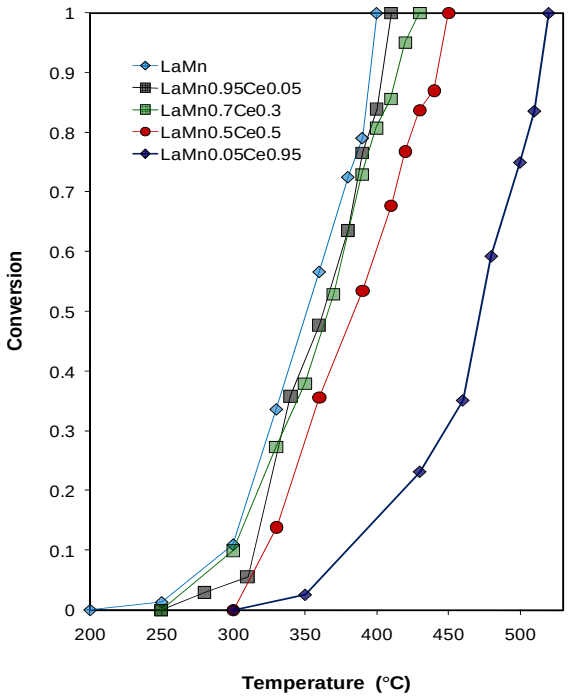

Figure 9: Light-Off Curves For Propane Combustion

Substituting cerium for lanthanum, while maintaining the manganese content at one cation per hexaaluminate unit, was also studied. In perovskites of the composition $La_{1-x}Ce_xMnO_3$, cerium doping has produced mixed results. Marchetti and Forni [29] found that $La_{0.9}Ce_{0.1}MnO_3$ was less active than $LaMnO_3$ for methane combustion. Song *et al.* [30] found that $La_{0.7}Ce_{0.3}MnO_3$ was less active than $LaMnO_3$ for methane combustion but more active for carbon monoxide combustion. Zhang-Steenwinkel *et al.* [31] found that for the range 0–0.3, the catalyst with x = 0.2 was most active for carbon monoxide oxidation. Alifanti *et al.* [32, 33] found that for the range 0–0.5, x = 0.1 provided the highest activity for methane combustion. Our experiments found that for $La_{1-x}Ce_xMnAl_{11}O_{19}$, cerium substitution increased activity, with maximum activity occurring at a higher cerium content (x = 0.4) than in the case

with perovskites, Figure 10. A substantial improvement of 30°C in both T_{50} and T_{100} over $LaMnAl_{11}O_{19}$ was achieved.

During the high-temperature stability test of $LaMnAl_{11}O_{19}$, using a self-sustained propane combustion reaction in a packed-bed reactor, a red-hot spot formed at the entrance of the reactor and remained stationary over 14 cumulative hours of operation and four start-ups. Light-off curves from before and after the test are displayed in Figure 11 and are virtually identical. Since the reactor was not within a tube furnace for these light-off curves, the reactor was not isothermal and the measured exit temperatures are lower than the reactor temperatures in Figures 9–11. This experiment confirmed that manganese-substituted hexaaluminates are both active and stable enough to be used as combustion catalysts.

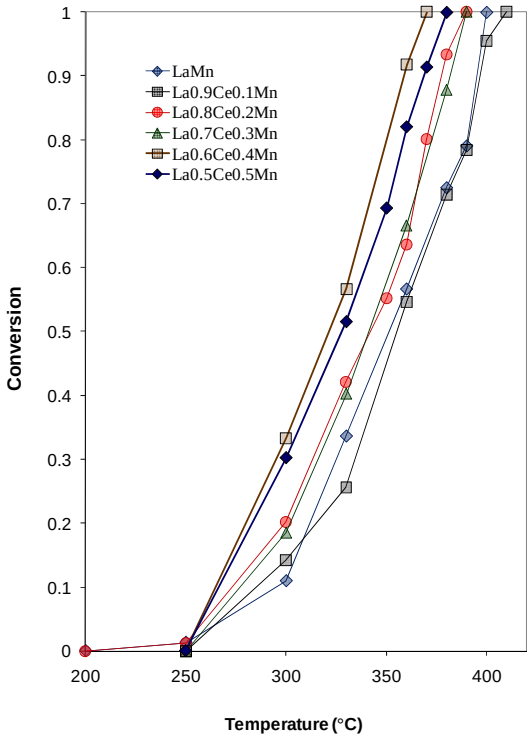

Figure 10: Light-Off Curves For Propane Combustion

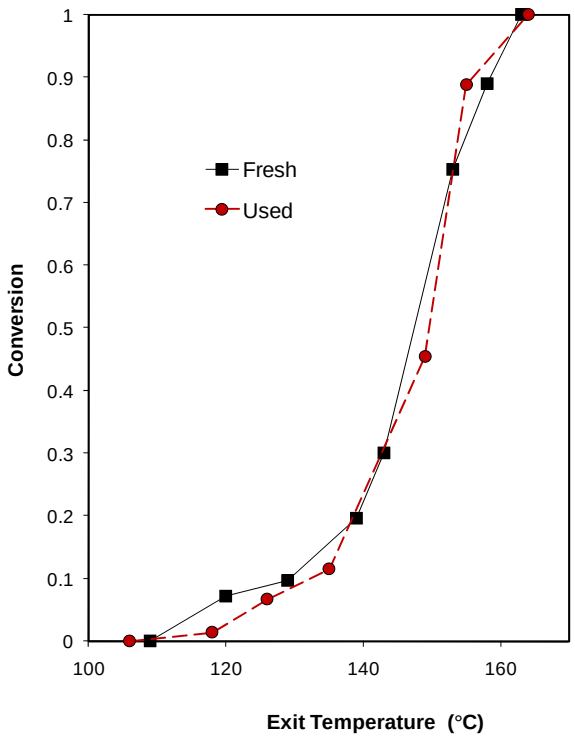

Figure 11: Light-Off Curves For $LaMnAl_{11}O_{19}$ Used In High-Temperature Stability Test

3.4 Flat Plate Steam Reformer Development

In this effort the application of the combustion catalyst in a compact steam reformer reactor was investigated. One consideration was to have a substrate which allowed a high surface area per unit volume while withstanding the intense thermal energy produced by fuel combustion. Since the steam reformer operates at 600-800 ^{O}C, the substrate materials have to survive at higher temperature than 800 ^{O}C. Foam metal substrate was chosen and the catalyst was washcoated to FeCrAlloy metal foam. FeCrAlloy was selected based on its high melting

point (1,500°C), long term creep strength, high corrosion resistance, large thermal conductivity, excellent compatibility between the metal substrate and the coated catalyst, and low cost. Therefore, a comparison between the performance of the hexaaluminate catalyst in pellet form and its performance coated on metal foam was carried out.

3.4.1 Experimental Procedure and Development Effort

3.4.1.1. Combustion Catalyst Coated Metal Foam Preparation: The catalyst supports FeCrAlloy foam strips (Porvair, 40pores/inch, 5% density, and 0.02" pore diameter) were washcoated with $La_{0.8}Ce_{0.2}MnAl_{11}O_{19}$ using the following procedure. The catalyst supports were sonicated in acetone for one hour, oxidized in air at 900°C for 24 hours to grow alumina scales for improved catalyst adhesion, dipped in 12% slurry of $La_{0.8}Ce_{0.2}MnAl_{11}O_{19}$ in ethanol, and dried with a heat gun. Three dipping/drying cycles were performed for each foam support. Figure 12 show both bare and coated metal foams using Dark Field Microscopy Imaging at 500X. The left image is for bare metal foam while the right image is for a coated piece. Looking at the coated piece, center hole, the grey catalyst preferentially coated near the edge is clearly shown.

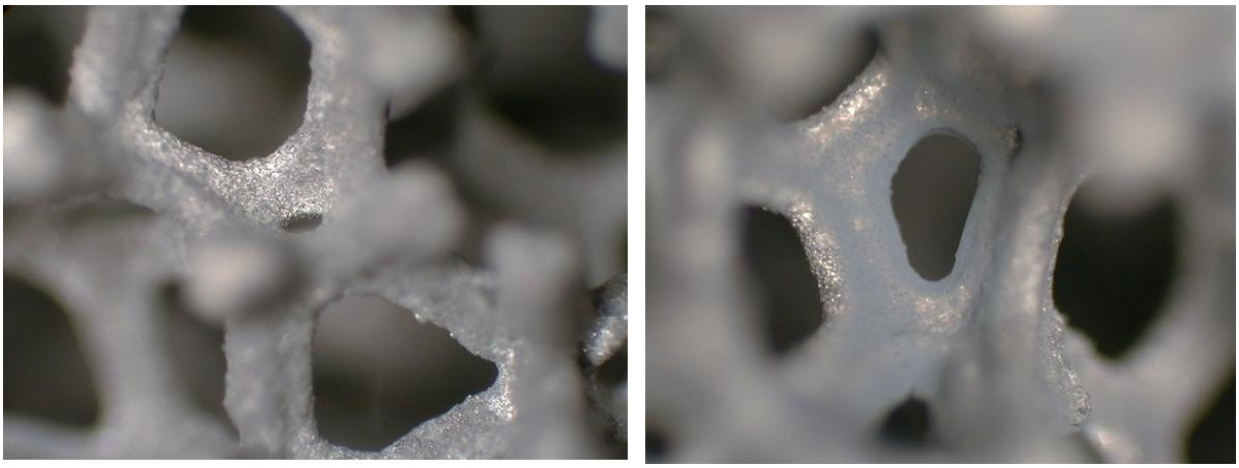

Figure 12: FeCrAlloy Foam – Bare (Left); Washcoated with Hexaaluminate Combustion Catalyst (Right) Using Dark Field Microscopy Imaging at 500X

3.4.1.2. Test Apparatus: The experimental efforts used several catalytically heated flat plate reactor designs. In the beginning, to investigate flat plate catalytic combustion characteristics, a reactor was constructed from two stainless steel plates each of dimensions 3in x 1.5in x 1/16in, and a stainless steel frame with dimension of 3in x 1.5in x 6/16in The stainless steel frame had a 2in x 6/16in x 6/16in cavity to house combustion catalyst. Two FeCrAlloy foam strip catalyst supports (Porvair, 40 pores/inch, 5% density, and 0.02" pore diameter) with dimensions 2in x 6/16in x 3/16in, stacked tightly inside the frame cavity. Pressure drop was measured at room temperature using compressed air and pressure transducers (Setra 209, range 0-1psi, accuracy ±0.02% of full scale). The flat plate reactor's performance was first characterized for the catalytic combustion of propane. 50sccm (standard cubic centimeters) propane and 1190sccm air (providing a stoichiometric fuel/air ratio) were fed to the reactor

without preheating. Combustion was initiated by resistively heating the reactor with coiled heat rope. Upon light-off, resistive heating was discontinued and the reactor was allowed to reach steady state. The temperature profile of the reactor was measured at four external points (corresponding to the bolt positions) in a line along the axis of flow with a type E thermocouple probe. The probe had a 1.5 mm diameter stainless steel sheath. The experiment was repeated with a feed of 14 ml/h JP-8 jet fuel (dispensed by an ISCO LC-5000 syringe pump) and 3630 sccm air. Using $C_{11}H_{21}$ as an approximate molecular formula for JP-8, this is calculated to be 72% excess air.

Based on the results of the flat plate combustion experiments, several steam reforming reactors were designed. In general, the flat plate steam reforming reactor was constructed from a matrix of stainless steel plates with and without cavities. The solid plates and those with cavities were staked in sequence to create a steam reforming channel flanked by two outer combustion channels in a parallel flow configuration, Figure 13. The steam reformer cavity housed steam reforming catalyst, Ru/n–CeO_2, coated on Recemat International Nickel-Chromium-Aluminum (Ni/Cr/Al) metal foam (17-23 pores/inch, 0.016" pore diameter). The combustion cavities housed the hexaaluminate combustion catalyst pellets, while for the metal foam experiments, two FeCrAlloy foam strip catalyst supports inserted inside the combustion cavities instead. The plates were bolted together, with Resbond 907GF 2,350°F (1,287°C) adhesive and sealing putty. After assembly, the reactor was fed 3000sccm air at 100 psi and found to be free of leaks detectable by Snoop Liquid Leak Detector (Swagelok).

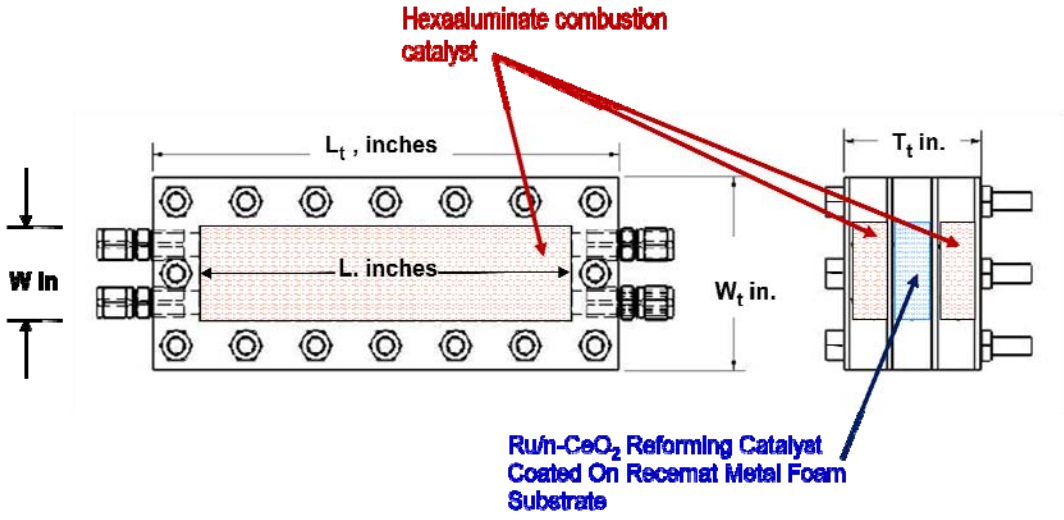

Figure 13: Flat-Plate Steam Reforming Reactor Flanked by Two Outside Combustion Reactors

The first reforming reactor had two 4" long x 1" wide x ½" thick cavities for combustion channels while reforming channel was 1cm thick, Figure 14. The length of the channel was in the direction of flow. The final reactor design had two 2" long x 11" wide combustion channels, using cross flow configuration to provide uniform temperature distribution along the 11" long x 2" wide reforming channel. For combustion light-off, a 28 AWG Ni/Cr heating wire in a 1/8” diameter McMaster high temperature nonporous high-alumina two-bore

ceramic tube was used in each combustion channel. The heating wire was activated until combustion started then deactivated.

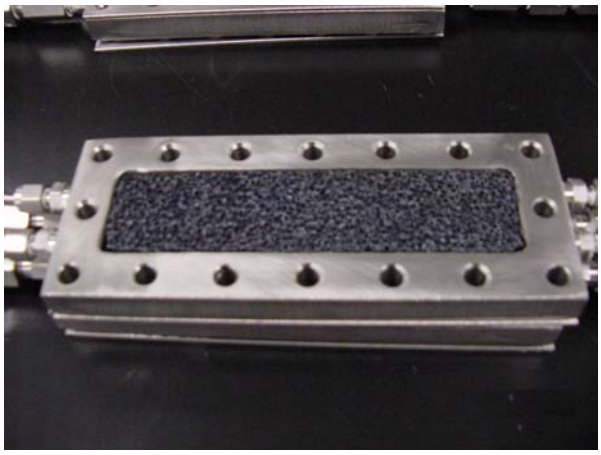

Figure 14: Flat Plate Catalytically Heated Steam Reforming Reactor

3.4.2 Results and Discussion

The flat plate combustion reactor using hexaaluminate catalyst coated on FeCrAlloy metal foam showed good performance at temperature ranges of 400-600^{o}C. Figure 15 shows that pressure drop is negligible for the operating flow rate range. Temperature profiles of the reactor exterior are shown in Figure 16. For propane combustion (lower heating value of 75 W), at 50sccm, the temperature was a rather uniform 480-490 °C over the first half of the reactor and then smoothly dropped to 417°C near the exit. For JP-8 (lower heating value of 133 W), at 14 ml/h, the hot band was 100 °C hotter, but was located in the mid-section of the reactor, as the JP-8 was not preheated and thus required some residence time to vaporize. The reactor burned propane for 7 hours and JP-8 for 27 hours with no sign of catalyst deactivation.

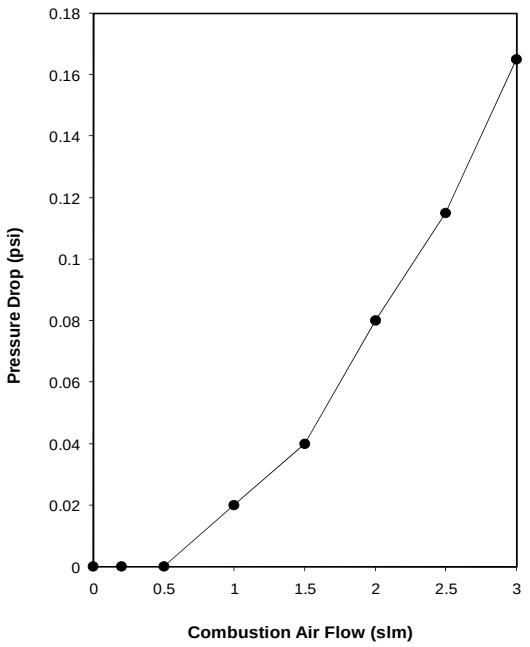

Figure 15: Parallel Plate Catalytic Combustion Reactor Pressure Drop Curve.

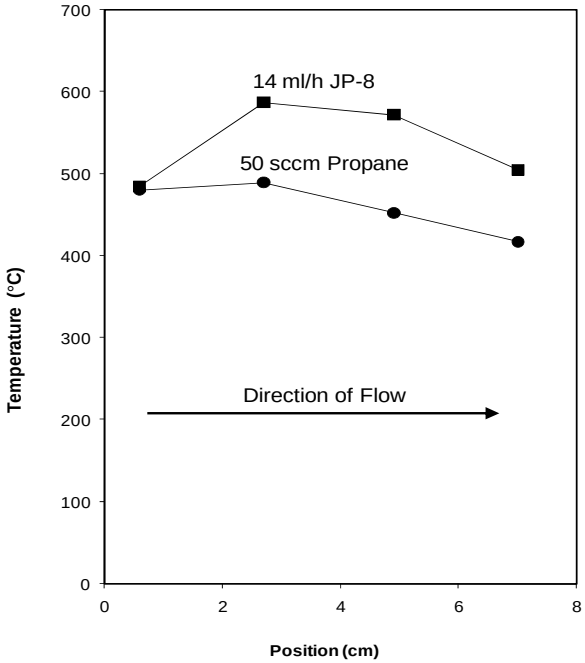

Figure 16: Temperature Profile of Parallel Plate Catalytic Combustion Reactor.

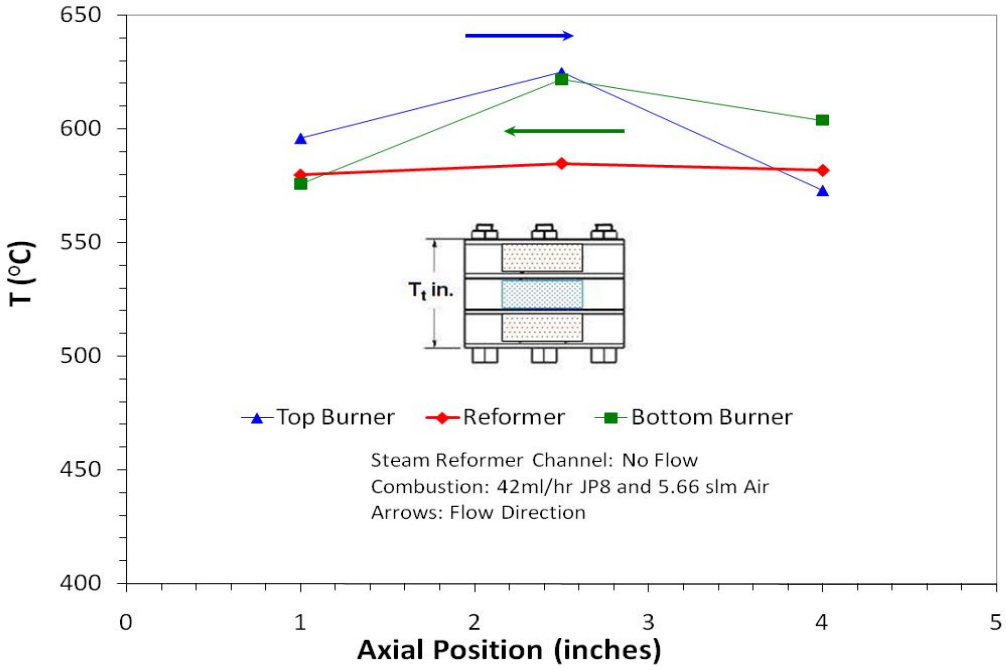

Figure 17: Flat Plate Temperature Distribution with no Reformer Channel Flow

The flat plate steam reforming reactor using catalyst coated metal foams (4"x1") in the combustion and reforming channels performed well in the temperature range up to 650°C. First it was tested with no fuel–steam mixture flowing into the reforming channel while feeding combustion channels total of 42ml/hr JP8 and 5.66 SLPM (standard liter per minute) combustion air. Figure 17 shows temperature distributions for JP-8 combustion. Combustion channels' temperature distribution ranges between 576°C to 625°C with reforming channel at a uniform temperature of 585°C. Figure 18 shows the steam reforming reactor temperature distributions for 0.1 g/min JP8 and 120°C 0.65gpm steam (steam to carbon ratio, S/C of 5) fed to the reformer channel while both combustion channels were fed 36ml/hr JP8 and 4.66 SLPM of air. The impact of the reforming reaction in the reformer channel is evident. The combustion channels temperature distribution is no longer symmetric around midpoint.

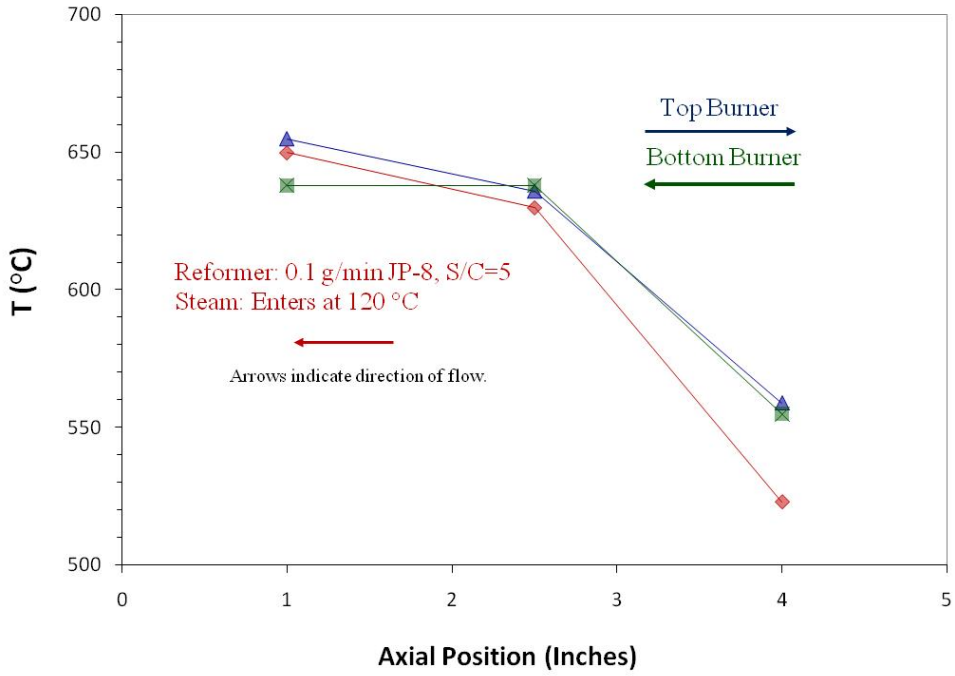

Figure 18: Flat Plate Temperature Distribution with Reformer Channel Flow

Keeping reaction temperatures low caused the formation of hydrocarbon aerosol, mixed with the reformate stream that was difficult to separate, while the need to eliminate the aerosol grew desperate when the analysis showed its high sulfur content. Increasing operating temperatures was necessary to reform high flow rate of JP8. Reforming channels operating temperatures needed to be at 800-850^{o}C to eliminate the formation of aerosol. Delivering reaction thermal energy at 800-850^{o}C required keeping combustion channels at higher than 1000^{o}C. This requirement proved fatal for the hexaaluminate catalyst coated on FeCrAlloy metal foam, as shown in Figure 19; it caused catalyst delamination and destroyed the FeCrAlloy substrate. For the high operating temperature ranges the new catalyst can be used in pellet form as long as the pressure drop is reasonable. Pumping combustion air at high pressure will drastically increase parasitic power. The investigation of the pressure drop revealed that although pellet form beds had twice the pressure drop as the combustion catalyst coated FeCrAlloy foam, the pressure drop is reasonable with maximum drop less than 1 psi, Figure 20.

Figure 19: Destroyed Hexaaluminate Combustion Catalyst coated FeCrAlloy Foam

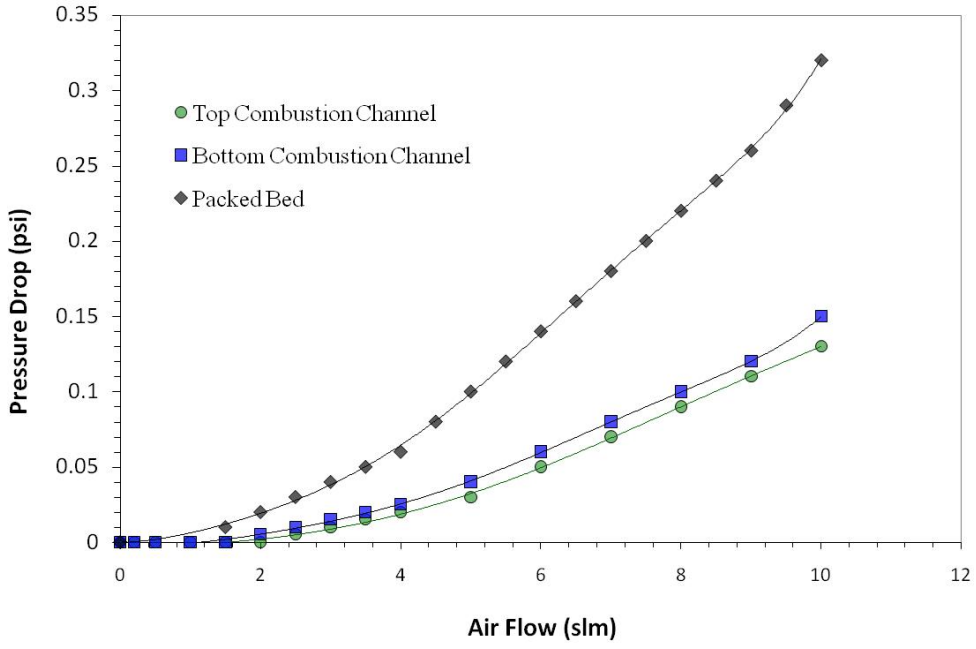

Figure 20: Combustion Channel Pressure Drop Comparison

Other parameters impacting the performance of the flat plate reactor include feeding liquid fuel instead of vapor to the combustion channels and the steam temperature fed to the reforming channel; both caused less than uniform temperature distribution. As seen from figures 16, 17, and 18, a large section of the entrance area of the combustion channel is used to evaporate the fuel resulting in a non-uniform temperature

distribution. While in the case of delivering steam at lower than the operating temperature of 800-850^{o}C, again large area in the entrance section of the reforming channel is used to bring the fuel-steam mixture to the operating temperature range. To effectively use the entire length of a reactor, liquid fuels have to be evaporated before entering a catalytic combustion chamber and the steam-fuel mix need to be delivered to the reforming channel at or near the operating temperatures.

The evaporation of combustion fuel resulted in 2 inches long red-hot spot formed at the entrance of the combustion channel and remained stationary over multiple cumulative hours of operation, start-ups, and different fuel flow rates, similar to those spots formed during the catalyst development efforts. The formation of the red-hot spot is an indication that combustion is carried out and the fuel is completely burned in the first two inches. To achieve uniform temperature distribution for the entire reactor, the reactor was redesigned as a cross flow heat exchanger. The combustion channels are 2" along fuel-air mixture flow direction and 11" wide, while the reforming channel is 11" along the fuel-steam mix flow direction and 2" wide, Figure 21. This flat plate design is capable of reforming JP8 to produce enough reformates for 1.5kW Solid Oxide Fuel Cell stack.

Figure 21: Cross Flow Steam Reforming Reactor

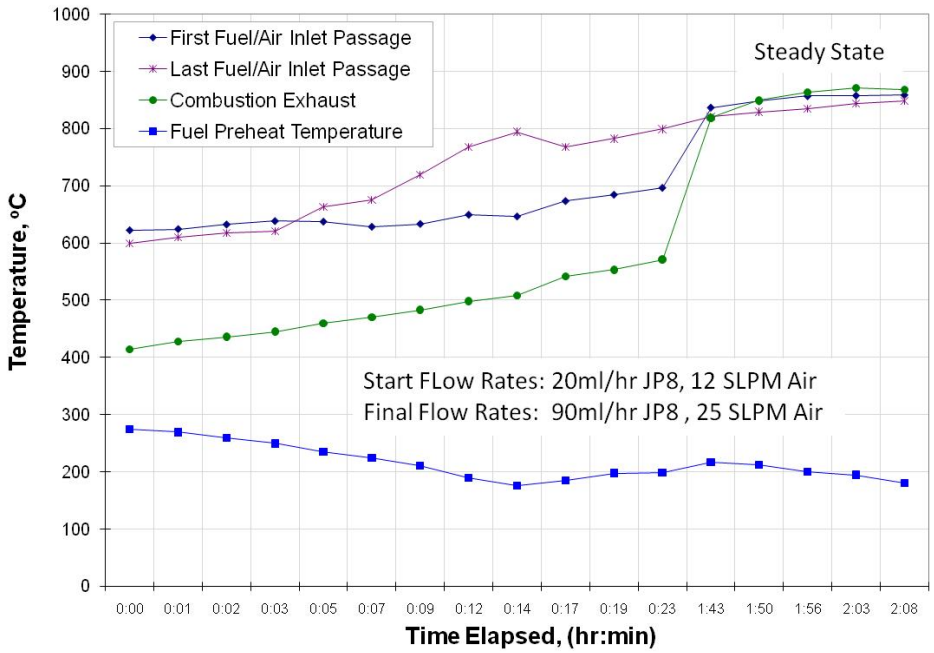

Figure 22: Temperature Distribution in the 2"x11" Reactor with No Reforming Channel Flow

The 2" x 11" combustion channel was tested to examine temperature distribution and determine whether hot spots would exist. Using only one side of the parallel plate cross-flow reactor, combustion catalyst in pellet form was used, electric heating was activated until reaching ignition temperature, then preheated fuel air mixture flowed into the combustion channels, combustion started and electric heating was deactivated. Fuel-air mixture gradually increased until it reached designated rate. Temperature measurements were taken at the inlet to the fuel-air manifold to measure preheat temperature, at the end of the first and last passages from the fuel-air manifold to catalyst bed to measure catalyst bed temperatures, and at the exit of the combustion channel to measure exit temperature. As shown in Figure 22, at steady state the cross-flow reactor gave a remarkable uniform temperature distribution along the reformer channel flow direction with maximum temperature deviation not more than $20^{O}C$. Visual examination showed no segregated hot spots existed while the entire reactor was one continuous orange hot spot.

The flat plate reactor design overcame three drawbacks of packed-bed reactors: high pressure drop, non uniform temperature distribution, and concentrated hot spots. The flat plate reactor using the developed combustion catalyst also allowed high heat flux, maximizing reaction intensity. As shown in Figure 23, $4.8W/cm^2$ heat flux was achieved for JP-8 while Charlesworth *et al.* [1] observed $1W/cm^2$ for methane combustion. Appendix B gives the procedure to calculate heat flux.

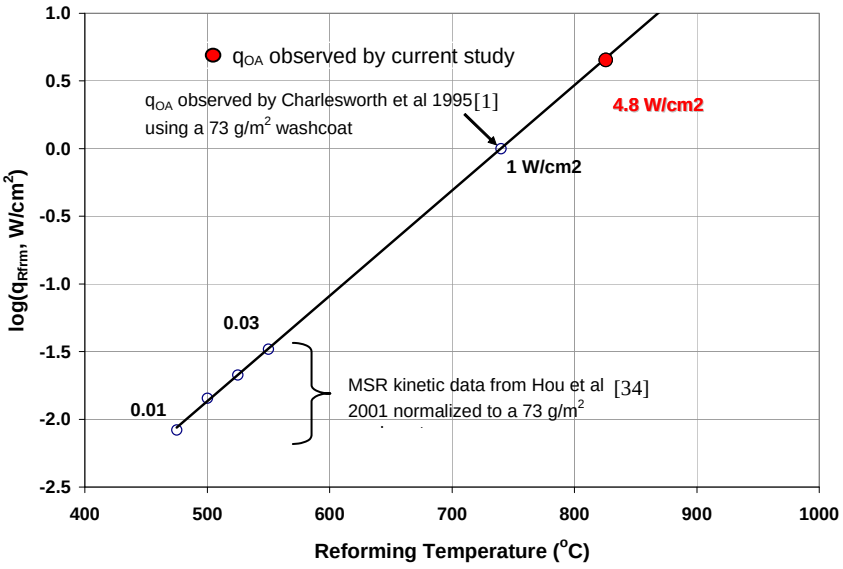

Figure 23: Catalytic Combustion Heat Flux Comparison In Flat Plate Reactors

4. CONCLUSION

4.1. Thin Film Coated Catalyst Proof of Concept

JP-8 catalytic cracking, in packed-bed and coated wall reactors, was studied at temperatures, pressures, and space velocities relevant to applications in compact fuel processor systems. Two different catalyst formulations, manganese supported on γ-alumina, and mixed MFI and BEA acidic zeolites, were compared in tubular packed bed reactors, and found to give similar cracking conversions at atmospheric pressure over a range of temperatures and space velocities. Greater than 80 wt% cracking conversion could be achieved with either catalyst at LHSV = 5.5 h^{-1} at mean reactor temperature < 250°C, while at LHSV = 44 h^{-1} mean reactor temperature of > 520°C was required. Tubular reactors with BEA zeolite catalyst coated on the tube inner wall achieved 80 wt% conversion at 100 h^{-1} liquid space velocity with reactor temperature < 380°C. Thin film coated catalyst reactors have the potential to process many times the fuel flow rate as similar volume packed-bed reactor while operating at lower temperatures.

4.2. Combustion Catalyst Development

The development of a substituted hexaaluminate combustion catalyst with high surface area (up to 78m^2/g) and withstanding extreme temperature was achieved. Hexaaluminates can be easily and inexpensively synthesized via a surfactant-mediated process. The better formulations combine high-temperature stability with activity sufficient to sustain catalytic combustion at lower temperatures. $La_{0.6}Ce_{0.4}MnAl_{11}O_{19}$ was the most active catalyst tested.

4.3. Flat Plate Steam Reformer Development

A parallel plate reactor using catalytic combustion with substituted hexaaluminate catalyst supported on FeCrAlloy foam successfully burned propane and JP-8. It exhibited a low pressure drop, a sufficiently-uniform temperature profile, and stable self-sustained operation. It performed well in temperature range of up to 650^{o}C. For extreme operating temperatures the hexaaluminate catalyst can be used in its pellet form with slightly higher pressure drop instead of the FeCrAlloy foam. The flat parallel plate catalytic combustion reactor design overcame three drawbacks of packed-bed reactors: high pressure drop, none uniform temperature distribution, and concentrated hot spots while allowing high heat flux.

Further testing effort is needed to characterize the performance of the parallel plate reactor. Relationships between fuel and steam flow rates, temperature distributions, conversion efficiencies, exhaust flue gases thermal energy, and partial loads are needed to determine design capabilities as well as catalysts' reliability.

APPENDIX A: Experimental Data Interpolation Using Least Square Technique

Table A-1 lists packed-bed MFI/BEA-PB reactor test results for four LHSV, while Table A-2 lists thin film coated catalyst BEA 2 channel reactor test results for one LHSV of $100h^{-1}$.

TABLE A-1: Packed-Bed MFI/BEA-PB Reactor Test Results

LHSV (h^{-1})	X (%)	RMT (^oC)	LHSV (h^{-1})	X (%)	RMT (^OC)
5.49451	17.2124	200.5	10.989	25.8186	310
5.49451	20.7389	201	10.989	27.7078	316
5.49451	19.0596	220	10.989	53.5264	329
5.49451	28.1276	218.5	10.989	52.3929	327.5
5.49451	65.4072	233	10.989	65.1134	348
5.49451	62.5525	232.5	10.989	73.6776	349
5.49451	83.3753	247	10.989	76.3224	355.5
5.49451	83.5432	247.5	10.989	72.5441	355
21.978	5.75147	397.5	43.956	16.2469	484
21.978	6.80101	400.5	43.956	12.5472	484
21.978	11.5239	409.5	43.956	41.1996	499
21.978	11.1041	410.5	43.956	37.4213	499.5
21.978	69.6683	432.5	43.956	64.6568	510.5
21.978	43.0101	433	43.956	62.2953	510.5
21.978	74.7061	446	43.956	79.4553	523
21.978	73.4467	447.5	43.956	79.6914	525.5

TABLE A-2: Thin Film Coated Catalyst BEA 2– Channel Reactor Test Results

LHSV (h^{-1})	X (%)	RMT (^OC)
100	16	339.5
100	53	360.5
100	85	379
100	83	375.5
100	65	366
100	28	344.5
100	8	342.5
100	26	370.5
100	79	389.5
100	70	376
100	48	375.5
100	66	385
100	71	392.5

Calculation Procedure

The purpose of this calculation is to find the liquid space velocity (LHSV, h^{-1}) for the packed-bed that matches the operating temperature and conversion efficiency ranges of the thin-film 2-channel reactor to facilitate a performance comparison between the two technologies.

Using *Multi–Polynomial Regression (MPR)* technique the packed–bed data in Table A-1 was curve fitted, as z a function of x and y, to several polynomials of the first (linear), second, third, fourth, fifth, and sixth degrees. Where *z* is the liquid space velocity (LHSV, h^{-1}), *x* is the reactor mean temperature (RMT, ^{O}C), and *y* is the cracking conversion efficiency (wt%). The values of the Residual Sum of Squares (RSS) for the different regressions are listed in Table A-3.

TABLE A-3: Values of the Regression Residual Sum of Squares (RSS)

Linear Regression	2nd Degree Polynomial Regression	3rd Degree Polynomial Regression	4th Degree Polynomial Regression	5th Degree Polynomial Regression	6th Degree Polynomial Regression
Residual Sum of Squares: RSS					
852.9435176	68.18344298	11.27697528	6.08038303	3.740075449	1.931247077

To select a good curve fit, the polynomial should have the least RSS while none of its zeros are within the data ranges. For each polynomial z was calculated for x range of 20 to 80 and for y range of 200 to 550. Plotting the resulted polynomials one can determine the optimum regression for the data set. Figure A-1 shows LHSV as a function of cracking conversion efficiency for RMT of 220°C for third, fourth, fifth, and sixth degree polynomials, while Figure A-2 shows LHSV as a function of reactor mean temperature (RMT) for 50% cracking conversion efficiency using the same four polynomials.

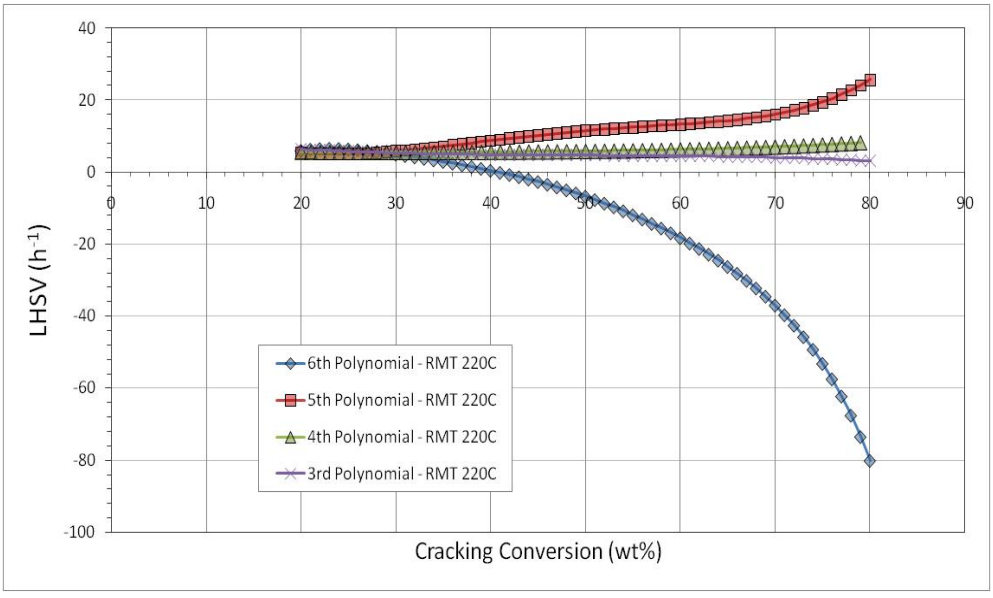

Figure A-1: LHSV vs Cracking Conversion Efficiency For RMT Of 220^{O}C Using Third, Fourth, Fifth, And Sixth Degree Polynomials

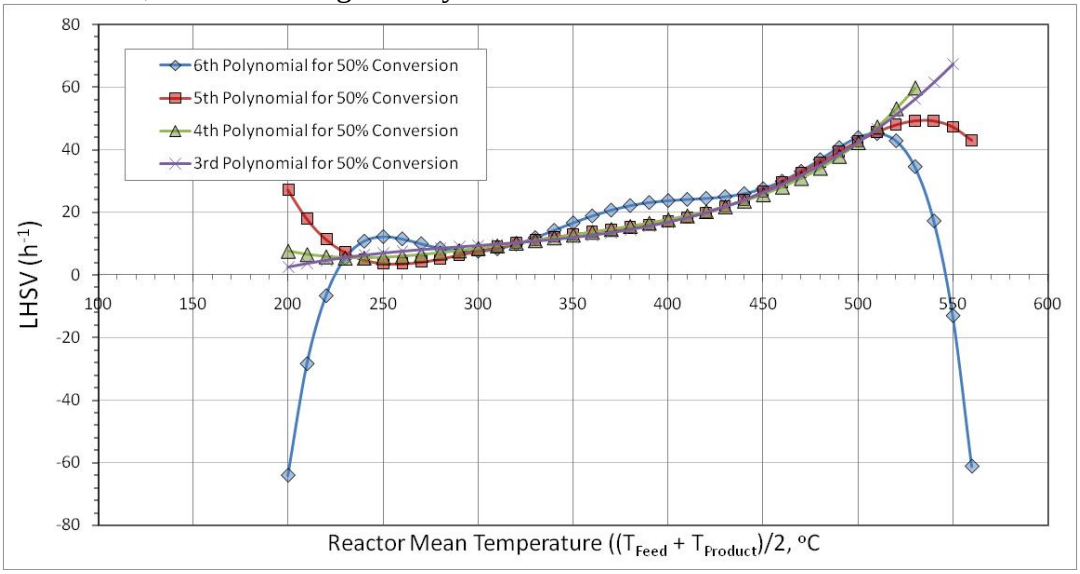

Figure A-2: LHSV vs RMT For Cracking Conversion Efficiency of 50% Using Third, Fourth, Fifth, And Sixth Degree Polynomials

From Figures A-1 and A-2 the fifth degree polynomial regression gave the least error, has no zeros in the data ranges, and resulted in the following equation:

$$z = 8.602058124*10^{-8}\,x^5 - 4.70840828*10^{-8}\,x^4\,y + 7.099288868*10^{-9}\,x^3\,y^2 - 2.127432215*10^{-9}\,x^2\,y^3 + 2.303451064*10^{-9}\,xy^4 - 3.819021883*10^{-10}\,y^5 + 6.152670546*10^{-7}\,x^4 + 3.467931174*10^{-6}\,x^3y + 1.352454025*10^{-6}\,x^2\,y^2 - 3.312952059*10^{-6}\,xy^3 + 6.139292214*10^{-7}\,y^4 - 1.253666951*10^{-3}\,x^3 - 6.677922582*10^{-4}\,x^2y + 1.78102944*10^{-3}\,xy^2 - 3.745415321*10^{-4}\,y^3 + 1.586922859*10^{-1}\,x^2 - 4.099667707*10^{-1}\,xy + 1.069250333*10^{-1}\,y^2 + 31.92095516\,x - 13.97679154\,y + 671.4121774 \qquad \text{(A-1)}$$

The fifth degree polynomial regression results are listed in Table A-4

TABLE A-4: Regression Analyses Using Fifth Degree Polynomial

Residual Sum of Squares: RSS = 3.740075463					
	X (%) x	RMT (^{o}C) y	LHSV (h^{-1}) z	Calculated z	Absolute Error
1.	20.7388749	201	5.494505495	5.477082779	0.017422715
2.	19.05961377	220	5.494505495	5.488713502	0.005791992
3.	28.12762385	218.5	5.494505495	5.525039261	0.030533766
4.	65.40722082	233	5.494505495	5.282743837	0.211761658
5.	62.55247691	232.5	5.494505495	5.691199338	0.196693843
6.	83.37531486	247	5.494505495	5.531771573	0.037266079
7.	83.54324097	247.5	5.494505495	5.485175234	0.00933026
8.	25.8186398	310	10.98901099	11.11533827	0.126327284
9.	27.70780856	316	10.98901099	10.88764791	0.101363077
10.	53.52644836	329	10.98901099	10.84783125	0.141179735
11.	52.3929471	327.5	10.98901099	10.77447758	0.214533411

12.	65.11335013	348	10.98901099	11.69062308	0.70161209
13.	73.67758186	349	10.98901099	10.25526612	0.733744871
14.	76.32241814	355.5	10.98901099	11.05966878	0.070657789
15.	72.5440806	355	10.98901099	11.41516521	0.426154224
16.	5.751469353	397.5	21.97802198	22.00392468	0.025902705
17.	6.801007557	400.5	21.97802198	21.9806034	0.002581422
18.	11.52392947	409.5	21.97802198	21.75988449	0.218137492
19.	11.10411419	410.5	21.97802198	22.12802478	0.150002799
20.	69.66834593	432.5	21.97802198	21.01022525	0.967796724
21.	43.01007557	433	21.97802198	22.18487356	0.206851578
22.	74.7061293	446	21.97802198	22.04562642	0.067604444
23.	73.44668346	447.5	21.97802198	22.64373807	0.665716092
24.	16.24685139	484	43.95604396	43.93920175	0.016842208
25.	12.54722922	484	43.95604396	43.97228136	0.016237408
26.	41.19962217	499	43.95604396	43.53383616	0.422207793
27.	37.42128463	499.5	43.95604396	44.2436167	0.287572743
28.	64.65680101	510.5	43.95604396	43.76913211	0.186911842
29.	62.29534005	510.5	43.95604396	44.27692605	0.320882093
30.	79.45528967	523	43.95604396	43.44235766	0.513686296
31.	79.69143577	525.5	43.95604396	44.38401573	0.427971777

To find an LHSV for the packed-bed reactor at the operating temperature and conversion efficiency for the thin film reactor, those values listed in Table A-2 were used in equation A-1. The calculated LHSV values were averaged as shown in Table A-5:

TABLE A-5: Backed-Bed LHSV at Thin Film Operating Parameters Range

Thin Film Coated Reactor			Packed-Bed Reactor
LHSV (h^{-1})	X (%)	RMT (^{O}C)	Calculated LHSV (h^{-1})
Z	***X***	***Y***	
100	16	339.5	14.91
100	53	360.5	13.96
100	85	379	15.27
100	83	375.5	14.31
100	65	366	14.04
100	28	344.5	11.42
100	8	342.5	20.17
100	26	370.5	12.49
100	79	389.5	15.27
100	70	376	14.57
100	48	375.5	14.59
100	66	385	15.97
100	71	392.5	16.20
Average LHSV			14.86

Therefore, a packed-bed's LHSV that matches thin film reactor performance is 14.86.

APPENDIX B: Heat Flux Calculations

BURNERS INPUT:

JP-8: Q_{JP8} = 210 ml/hr
Molar Mass (M_{JP8}) = 153 g/mol
Density (ρ_{JP8}) = 0.8 g/ml
Air : Q_{air} = 54 SLPM
N_2 flow rate (Q_{N2}) = 0.79 Q_{air} = 42.66 SLPM
O_2 flow rate (Q_{O2}) = 0.21 Q_{air} = 11.34 SLPM

Molar Mass Flow Rate:
JP-8 (m_{JP8}) = $Q_{JP8}\,\rho_{JP8}/M_{JP8}$ = 0.018300654 mol/min
N_2 (m_{N2}) = Q_{N2}/[0.0820574587*273.15] = 1.903275177 mol/min
O_2 (m_{O2}) = Q_{O2}/[0.0820574587*273.15] = 0.505933908 mol/min

Temperature: 609^oK

BURNER OUTPUT:

Molar Mass Flow Rate:
H_2O (m_{H2O}) = 10.5 m_{JP8} = 0.192156863 mol/min
O_2 (m_{O2}) = m_{O2} – 16.25 m_{JP8} = 0.208532619 mol/min
N_2 (m_{N2}) = 1.903216235 mol/min
CO_2 (m_{CO2}) = 11 m_{JP8} = 0.20130719 mol/min

Temperature:1000^oK

Heat of combustion (ΔH_C) = 6548 m_{jp8}/60 = 1.997211329 kW

Enthalpy of Combustion Gases:

Gases	Burner Input H_{609K} kJ/mol	Burner Output H_{1000K} kJ/mol	Enthalpy Gain* **ΔH** kW
O_2 (H_{O2})	18.213	31.386	0.045786776
N_2 (H_{N2})	17.835	30.135	0.390171411
CO_2 (H_{CO2})	35.632	55.706	0.067350675
H_2O (H_{H2O})	56.694	71.893	0.048676536
Total Gain (ΔH_T)			0.551985399

*$\Delta H = 60\, m_{gas}(H_{1000K} - H_{609K})$

Heat Input (Q_{in}) = [1000 ($\Delta H_C - \Delta H_T$) /surface area of the combustion channels]
= 5.091201665 W/cm2
Radiation Losses (R_L) = 0.3054721 W/cm2
Heat Flux = Q_{in} - R_L = 4.785729565 W/cm2

REFERENCES

1. R. Charlesworth, A. Gough, C. Ramshaw, "Combustion And Steam Reforming Of Methane On Thin Layer Catalysts For Use In Catalytic Plate Reactors," 4th UK/National Conference on Heat Transfer, Institution of Mechanical Engineers, 26-27 September (1995) 85-89.
2. H. Arai, M. Machida, " Thermal Stabilization Of Catalyst Supports And Their Application To High-Temperature Catalytic Combustion," Applied Catalysis A: General 138 (1996) 161-176.
3. L.-C. Yan, L.T. Thompson, "Synthesis And Characterization Of Aerogel-Derived Cation-Substituted Barium Hexaaluminates," Applied Catalysis A: General 171 (1998) 219-228.
4. B.W.-L. Jang, R.M. Nelson, J.J. Spivey, M. Ocal, R. Oukaci, G. Marcelin, "Catalytic Oxidation Of Methane Over Hexaaluminates And Hexaaluminate-Supported Pd Catalysts," Catalysis Today 47 (1999) 103-113.
5. H. Inoue, K. Sekizawa, K. Eguchi, H. Arai, "Thick-Film Coating Of Hexaaluminate Catalyst On Ceramic Substrates For High-Temperature Combustion," Catalysis Today 47 (1999) 181-190.
6. Y.S. Seo, S.J. Cho, S.K. Kang, H.D. Shin, "Experimental And Numerical Studies On Combustion Characteristics Of A Catalytically Stabilized Combustor," Catalysis Today 59 (2000) 75-86.
7. P. Artizzu-Duart, J.M. Millet, N. Guilhaume, E. Garbowski, M. Primet, "Catalytic Combustion Of Methane On Substituted Barium Hexaaluminates," Catalysis Today 59 (2000) 163-177.
8. E. Pocoroba, E.M. Johansson, S.G. Jaras, "Aging Of Palladium, Platinum And Manganese-Based Combustion Catalysts For Biogas Applications," Catalysis Today 59 (2000) 179-189.
9. L. Lietti, C. Cristiani, G. Groppi, P. Forzatti, "Preparation, Characterization And Reactivity Of Me-Hexaaluminate (Me=Mu, Co, Fe, Ni, Cr) Catalysts In The Catalytic Combustion Of NH3-Containing Gasified Biomasses," Catalysis Today 59 (2000) 191-204.
10. M. Ocal, R. Oukaci, G. Marcelin, B.W.-L. Jang, J.J. Spivey, "Steady-State Isotopic Transient Kinetic Analysis On Pd-Supported Hexaaluminates Used For Methane Combustion In The Presence And Absence Of NO," Catalysis Today 59 (2000) 205-217.
11. T.J. Campbell, A.H. Shaaban, F.H. Holcomb, R. Salavani, M.J. Binder, "JP-8 Catalytic Cracking For Compact Fuel Processors," Journal of Power Sources 129 (2004) 81-89.
12. P-O.F. Andersson, M. Pirjamali, S.G. Jaras, M. Boutonnet-Kizling, "Cracking Catalysts Additives For Sulfur Removal From FCC Gasoline," Catalysis Today 53 (1999) 565-573.
13. A.E.W. Beers, T.A. Nijhuis, F. Kapteijn, "European Commission Project No. GRD1 CT1999 10596: Intelligent Column Internals For Reactive Separations," Deliverable No. 25, Workpackage 6, December 2000.
14. N. Kirshen, "The Determination of Sulfur Gases in Natural Gas with Pulsed Flame Photometric Detector (PFPD)," Varian GC Application Note Number 60, http://www.varianinc.com.
15. K. Venkataraman, J.M. Redenius, L.D. Schmidt, "Millisecond Catalytic Wall Reactors: Dehydrogenation Of Ethane," Chemical Engineering Science 57 (2002) 2335-2343.

16. S.J. Cho, Y.S. Seo, K.S. Song, N.J. Jeong, S.K. Kang, “Surfactant-Mediated Synthesis Of Metal Substituted Hexaaluminate Fromalumina Sol,” Applied Catalysis B: Environmental 30 (2001) 351-357.
17. J. Wang, Z. Tian, J. Xu, Y. Xu, Z. Xu, L. Lin, “Preparation Of Mn Substituted La-Hexaaluminate Catalysts By Using Supercritical Drying,” Catalysis Today 83 (2003) 213-222.
18. G. Groppi, C. Cristiani, P. Forzatti, “Preparation, Characterisation, And Catalytic Activity Of Pure And Substituted La-Hexaaluminate Systems For High-Temperature Catalytic Combustion,” Applied Catalysis B: Environmental 35 (2001) 137-148.
19. S. Imamura, A. Doi, S. Ishida, “Wet Oxidation Of Ammonia Catalyzed By Cerium-Based Composite Oxides,” Ind. Eng. Chem. Prod. Res. Dev. 24 (1985) 75-80.
20. S. Imamura, M. Nakamura, N. Kawabata, J.-I. Yoshida, S. Ishida, ”Wet Oxidation Of Poly(Ethylene Glycol) Catalyzed By Manganese-Cerium Composite Oxide,” Ind. Eng. Chem. Prod. Res. Dev. 25 (1986) 34-37.
21. S. Imamura, Y. Okumura, T. Nishio, K. Utani, Y. Matsumura, ”Wet-Oxidation Of A Model Domestic Wastewater On A Ru/Mn/Ce Composite Catalyst,” Ind. Eng. Chem. Res. 37 (1998) 1136-1139.
22. H. Chen, A. Sayari, A. Adnot, F. Larachi, “Composition-Activity Effects Of Mn-Ce-O Composites On Phenol Catalytic Wet Oxidation,” Applied Catalysis B: Environmental 32 (2001) 195-204.
23. T.J. Campbell, A.H.Shaaban, F.H.Holcomb, R. Salavani, M.J.Binder,”JP-8 Catalytic Cracking for Compact Fuel Processors,” J. of Power Sources 129 (2004) 81–89
24. P-O.F. Andersson, M. Pirjamali, S.G. Jaras, and M. Boutonnet-Kizling, “Cracking catalyst additives for sulfur removal from FCC gasoline,” *Catalysis Today*, **53**, 1999, p 565-573.
25. A.E.W. Beers, T.A. Nijhuis, and F. Kapteijn, European Commission Project No. GRD1 CT1999 10596: *Intelligent Column Internals for Reactive Separations*, Deliverable No. 25, Workpackage 6, December 2000.
26. *Handbook of Aviation Fuel Properties*, Coordinating Research Council, Inc., Report No. 530, 1983.
27. D.R. Sobel, and L.J. Spadaccini, *Development of endothermic potential of JP-8*, U.S. Air Force Materiel Command Report WL-TR-2059, January 1994.
28. K. Venkataraman, J.M. Redenius, and L.D. Schmidt, “Millisecond catalytic wall reactors: dehydrogenation of ethane,” *Chem. Eng. Sci*., **57**, 2002, p 2335-2343.
29. L. Marchetti, L. Forni, “Catalytic Combustion Of Methane Over Perovskites,” Applied Catalysis B: Environmental 15 (1998) 179-187.
30. K.-S. Song, H.X. Cui, S.D. Kim, S.-K. Kang, “Catalytic Combustion of CH4 and CO on La1-xMxMnO3 Perovskites,” Catalysis Today 47 (1999) 155-160.
31. Y. Zhang-Steenwinkel, J. Beckers, A. Bliek, “Surface Properties And Catalytic Performance In CO Oxidation Of Cerium Substituted Lanthanum-Manganese Oxides,” Applied Catalysis A: General 235 (2002) 79-92.
32. M. Alifanti, R. Auer, J. Kirchnerova, F. Thyrion, P. Grange, B. Delmon, “Activity In Methane Combustion And Sensitivity To Sulfur Poisoning of La1-xCexMn1-yCoyO3 Perovskite Oxides,” Applied Catalysis B: Environmental 41 (2003) 71-81.

33. M. Alifanti, J. Kirchnerova, B. Delmon, “Effect Of Substitution By Cerium On The Activity Of LaMnO3 Perovskite In Methane Combustion,” Applied Catalysis A: General 245 (2003) 231-244.
34. Hou, K., and R. Hughes “The kinetics of methane steam reforming over a Ni/α-Al_2O_3 catalyst”, *Chem. Eng. J.*, Vol. 82, pp. 311-328 (2001).